A cell cycle-dependent GARP-like transcriptional repressor regulates the initiation of differentiation in *Giardia lamblia*

Han-Wei Shih, Germain C.M. Alas, Alexander R. Paredez

Department of Biology, University of Washington, Seattle, Washington 98195

Abstract

Transcriptional regulation of differentiation is critical for parasitic pathogens to adapt to environmental changes and regulate transmission. In response to encystation stimuli, *Giardia lamblia* cells shift from G1+S phase of the cell cycle to G2+M. By 2-4 hours, cyst wall proteins are upregulated, indicating that key regulatory steps occur within the first four hours of encystation. However, all characterized transcription factors (TFs) in *Giardia* have only been investigated at later time points of encystation. How TFs initiate encystation and link it to the cell cycle remains enigmatic. Here, we systematically screened six putative early upregulated TFs for nuclear localization, established their dynamic expression profiles, and determined their functional role in regulating encystation. We found a critical repressor, GLP4 that increases rapidly after 30 min of encystation stimuli and downregulates encystation specific markers, including Cyst Wall Proteins (CWPs) and enzymes in the cyst N-acetyl galactosamine (GalNAc) pathway. Depletion of GLP4 increases cyst production. Importantly, we observe that G2+M cells exhibit higher levels of CWP1 resulting from the activation of MYB2, a TF previously linked to encystation in *Giardia*. GLP4 upregulation occurs in G1+S cells, suggesting a role in repressing MYB2 and encystation specific genes in the G1+S phase of the cell cycle. Furthermore, we demonstrate that depletion of GLP4 upregulates MYB2 and promotes encystation while overexpression of GLP4 downregulates MYB2 and represses encystation. Together, these results suggest that *Giardia* employs a dose-dependent transcriptional response that involves the cell cycle regulated repressor GLP4 to orchestrate MYB2 and entry into the encystation pathway.

Importance:

Transition between life cycle stages is a common feature among parasitic pathogens and its regulation must be optimized to balance persistence of infection with transmission. The early transcription factors (TFs) regulating commitment to differentiate are totally unknown in *Giardia*. In this work, we identified GLP4, a previously uncharacterized GARP-like TF, as an early-acting transcriptional repressor that inhibits G1+S cells from entering the encystation pathway. GLP4 is therefore a key regulator controlling the balance between proliferative growth and terminal differentiation into infective cysts.

Introduction

To cope with environmental change, protozoa from all eukaryotic supergroups differentiate to dormant walled cysts, a process which is commonly called encystation (1). Deposition of a cyst wall to form water-resistant cysts allows parasitic protozoa to persist in fresh water and successfully transmit infection to susceptible hosts via a fecal-oral route. *Giardia lamblia* (synonymous with *Giardia duodenalis* and *Giardia intestinalis*) is a major cause of protozoan-based diarrhea and its encystation pathway plays an important role in pathogen virulence. *Giardia* exhibits a simple biphasic life cycle, consisting of cysts and trophozoites. *Giardia* infection occurs through consuming infectious cysts from contaminated water (2), food, or interpersonal contact (3). Following passage of cysts through the acidic environment of the stomach, vegetative trophozoites excyst in the duodenum and rapidly colonize the small intestine(4). In the small intestine, cell density, lipid starvation, and alkaline pH trigger a portion of trophozoites to initiate encystation (5-8). During the early stage of *Giardia* encystation, major morphological changes occur that include biogenesis of the Golgi-like Encystation Specific Vesicles (ESVs), Encystation Carbohydrate-positive Vesicles (ECVs), cell cycle arrest, and cytoskeleton rearrangement (5, 6, 9). *Giardia*'s cyst wall is composed of 37% cyst wall proteins (CWPs) and 63% carbohydrate filaments which are mainly made up by a [D-GalNAc-β(1-3)-D-GalNAc]$_n$ homopolymer (10-12). The expression levels of CWP1-3 are upregulated at 2-4 h post induction of encystation (13-15). The enzymes involved in the synthesis of β(1-3) GalNAc homopolymer, including GlcN 6-P isomerase (G6PI-B), GlcN 6-P N-acetylase (GNPNAT), phosphoacetylglucosamine mutase (PGM), UDP-GlcNAc pyrophosphorylase (UAP), UDP-GlcNAc 4'-epimerase (UAE) are upregulated at 10-18h post induction of encystation (10, 11, 13, 15).

Cell cycle arrest appears to be a common theme in encystation. Studies in *Giardia lamblia* (16), *Acanthamoeba* (17), and *Entamoeba invadens* (18) have all shown that encystation stimuli correlate with the accumulation of G2+M cells in the early stage of encystation. In *Acanthamoeba*, encystation frequency correlates with the proportion of cells arrested at G2(17), suggesting that differentiation may be initiated from G2+M cells. In *Giardia*, aphidicolin-treated trophozoite exhibited more ESVs in response to encystation stimuli. These observations led to a hypothesis that there is also a decision point in *Giardia*'s cell cycle that limits encystation to cells in G2+M (16, 19).

A recent study has shown that a Myeloblastosis domain protein (MYB) transcription factor (TF) is a master regulator of differentiation in *Toxoplasma gondii* (20). MYB TFs also modulate encystation in *Giardia* (21) and *Entamoeba* (22). Proteomic and RNA sequencing studies agree that *Giardia*'s MYB2 TF is a key regulator of encystation (14, 23, 24). In *Giardia*, several TFs have been characterized, including GARP-like protein 1 (GLP1, named for, Golden2, ARR-B, Psr-1 like protein 1) (25), E2 promoter binding factor 1 (E2F1)(26), WRKYGQK domain proteins (WRKY) (27), Paired box proteins 1,2 (PAX1,2)(28, 29), AT rich interaction domain (ARID) protein 1 (30), and MYB2. Thus far, all *Giardia* TFs which have been identified to regulate encystation activate

76 CWPs (21, 25-27, 29, 30). Interestingly, no single repressor has been identified, but promoter
77 analysis studies have suggested the presence of repressor binding sites in CWP2 and G6PI-B
78 (31-33).

79 The identification of TFs regulating entry into the encystation pathway is critical for
80 understanding how the initiation of differentiation is controlled. In *Giardia*, cell cycle arrest and
81 CWP1 upregulation occur 2-4 h post induction of encystation. Thus far, functional studies of
82 *Giardia's TFs* have focused on transcriptional regulation 24 h after inducing encystation. The
83 regulatory mechanism of TFs involved in the initiation of encystation and the spatiotemporal
84 dynamic of TF expression at the earliest stage of encystation remain unclear. Here, we
85 addressed these questions by screening putative TFs identified in a previous RNAseq study (14).
86 We determined the expression profiles of 6 TFs upregulated early in encystation, investigating
87 their functional roles by knockdown using CRISPRi and CasRX approaches, which led to the
88 identification and characterization of GLP4, a cell cycle-regulated repressor of encystation. Our
89 findings provide the first evidence of TF dynamics at 30 min to 4 h post induction of
90 encystation. We establish a key molecular link between encystation initiation and GLP4
91 expression that indicates GLP4 is a cell cycle-dependent repressor that inhibits the entry into
92 encystation by repressing MYB2 expression in G1+S cells.

93

94 **Results**

95 **Characteristics of transcription factors during early encystation in *Giardia***

96 Given that CWP1-3 are canonical encystation indicators in *Giardia (5, 6, 15, 23, 34)*, we first
97 investigated CWP1-3 protein levels during encystation initiation using NanoLuc reporters (35,
98 36). CWP1-3 protein levels began to increase after 1.5 h and rose exponentially by 4 h after
99 exposure to encystation medium (Fig. 1A). To date, several TFs have been identified with roles
100 in regulating CWP1-2; these include MYB2 (21), E2F1 (26), PAX1-2 (28, 29), ARID1(30) and
101 WRKY (27). Whether these TFs have a role in initiating entry into the encystation pathway has
102 not been established. The increase of CWPs is likely to be signaled through early response TFs,
103 which trigger the activation or repression of encystation specific genes. A previous
104 transcriptomics study identified 6 TF candidates that are upregulated within 4 h of encystation
105 (14). We sought to test whether these TFs function as upstream regulators of encystation. We
106 expressed these 6 proteins as mNeonGreen (mNG)-fusion to verify nuclear localization during
107 early encystation, using MYB2 as a positive control. MYB2 expression has been detected as
108 early as 7 h post induction of encystation in proteomic (23) and RNA sequencing studies (14).
109 We were able to detect nuclear localization of MYB2 at 4 h but not at 0 and 1.5 h (Fig. 1B). In
110 contrast, we observed 6 TFs, including MYB1, GLP3, GLP4, PAX1, ARID2, and E2F1 with nuclear
111 localization at 0 and 1.5 h of encystation stimulus (Fig. 1C; Fig. S1). MYB1 and GLP4 have not
112 been previously studied. We verified that MYB1-mNG and GLP4-mNG localized to the nuclei by
113 co-localization with the fluorescent DNA dye DRAQ5 (Fig. 1C).

114 We then decided to investigate the expression level of these TFs. GLP4 and MYB1 rose nearly
115 three-fold after 1.5 h of inducing encystation, with GLP4 having the highest level of
116 upregulation (Fig. 1D). Expressions of GLP3, PAX1, ARID2 and E2F1 only modestly increased by 4
117 h (Fig. S2A). Notably, MYB1 and GLP4 are upregulated before MYB2. This hints that these
118 transcription factors may be early encystation regulators upstream of MYB2 and CWP1.

119

120 **Depletion of MYB2 and GLP4 alter cyst production**

121 We next screened for knockdown constructs that would allow us to test the role of the six TFs
122 in regulating encystation. We tested the knockdown efficacy of an established dCas9-based
123 CRISPRi knockdown system (34) and generated a complementary CasRX knockdown system (37)
124 that targets mRNA for degradation (Fig. S3). Based on endogenously-tagged NanoLuc reporter
125 fusions for each of the TFs, we were able to significantly knockdown all six TFs of interest (Fig.
126 S4). Subsequently, we tested the most efficacious knockdown constructs for their ability to alter
127 CWP1 expression.

128 Previous studies have suggested a critical role for MYB2 in controlling *Giardia* encystation (21,
129 38); therefore, we investigated the phenotype of a CRISPRi-mediated MYB2 knockdown mutant
130 (Fig. 2A). Depletion of MYB2 reduced CWP1 and CWP2 levels at 4h of encystation (Fig. 2B-C; Fig.
131 S6E) and totally abolished the cyst maturation (Fig. 2D; Fig. S7A), confirming that MYB2 is
132 essential for encystation. Notably, our MYB2 CRISPRi cell line has better performance than a
133 previously reported MYB2 antisense silencing mutant that only partially reduced cyst
134 production (21). E2F1 (Fig. S5A-C) and PAX1 (Fig. S5D-F) have also been reported to regulate
135 CWP levels (26, 29), in agreement, we found that their knockdowns reduced CWP1 levels.

136 The functional role of ARID2, MYB1, and GLP4 in encystation has not been previously
137 established. Knockdown of ARID2 did not alter CWP1 levels (Fig. S5G-I) nor change the portion
138 of cells that enter the encystation pathway (Fig. S6C). Knockdown of MYB1 (Fig. 2E) resulted in
139 lower CWP1 levels (Fig. 2F), lower CWP2 levels (Fig. S6E), and fewer encysting cells at 4 h (Fig.
140 S6D); however, after 48 h the percentage of viable mature cysts (Fig. 2H; Fig. S7B-C) was similar
141 to the control. This suggests that MYB1 might be an upstream regulator of CWP1 but ultimately
142 it is not a major factor in cyst maturation. Interestingly, depletion of GLP4 (Fig. 2I) resulted in a
143 two-fold increase in CWP1 levels (Fig. 2J-K) and an approximately 20% increase in CWP2 levels
144 (Fig. S6E). Notably, GLP4 knockdown resulted in more mature cysts (Fig 2L) without changing
145 cyst viability (Fig. S7D-E). In summary, these results show that GLP4 is a repressor of CWP1 and
146 cyst development and, that while MYB1 is an activator of CWP1, it is not essential for cyst
147 maturation.

148

149 **Depletion of GLP4 upregulates the expression of encystation markers**

150 To further characterize the role of GLP4, we investigated whether depletion of GLP4 changes
151 cell growth rate and cell viability. Knockdown of GLP4 did not alter proliferation or viability
152 using the ATP-dependent click beetle green 99 (CBG99) luciferase assay (Fig S8A-B)(39). In
153 addition to the high bile Uppsala encystation method used above, *Giardia* can be encysted with
154 additional methods. These include the two-step method that removes bile and then provides
155 bile levels moderately above the critical concentration for bile acid micelle formation to
156 sequester cholesterol or cells can be starved for cholesterol with lipo-protein deficient media
157 (40). Similar to the high bile Uppsala method, both two-step and lipo-protein deficient
158 encystation media upregulated CWP1 more in the GLP4 mutant background (Fig. S8C),
159 indicating that the GLP4 knockdown phenotype is not restricted to a specific encystation
160 protocol. Considering that GLP4 has an important role in regulating encystation, we examined
161 how its levels change over a fine time course at the induction of encystation. Remarkably, GLP4
162 levels rapidly increased by 30 min while MYB1 did not appreciably ramp up until after 60 min of
163 encystation (Fig. 3A). GLP4 mutants have consistently higher CWP1 levels during early
164 encystation (Fig. 3B). We analyzed individual cells to determine whether the increase of CWP1
165 in the GLP4 knockdown lines was due to increased numbers of cells entering the encystation
166 program or resulted from increased levels of CWP1 per cell. We collected encysting cells from
167 different time points of encystation and stained with a CWP1 antibody to quantify encysting
168 cells. We then investigated various phenotypes of CWP1 trafficking in GLP4 mutants. The
169 percentage of encysting cells was 1.5-2 fold higher in GLP4 mutants at 0, 2, 4, and 24 h
170 treatments (Fig. S9; Fig. 3C-D). Furthermore, we analyzed CWP1-positive vesicle size and
171 volume to address whether CWP1 trafficking is altered as a result of increased CWP1 expression
172 in the GLP4 mutant. Our results show that neither vesicle size nor vesicle volume are changed
173 (Fig. 3E-F; Fig. S8D). This indicates that the increased levels of CWP1 are due to more cells
174 entering the encystation pathway. In contrast, overexpression of GLP4 inhibits 50% of CWP1
175 expression (Fig. S8E-G).

176 Because cyst wall composition includes 67% N-acetyl-D-galactosamine (GalNAc) homopolymers,
177 we sought to analyze whether GLP4 and MYB2 regulate other encystation markers, such as
178 enzymes in the GalNAc pathway (11). *In vivo* transcriptional regulation identified GNPNAT and
179 UAE as highly expressed enzymes in the GalNAc pathway (15). Additionally, MYB2 was shown to
180 modulate G6PI-B (41). Using NanoLuc as a reporter, we analyzed the expression level of G6PI-B,
181 UAE, and GNPNAT at 0, 1.5, 4, 7, 18, and 24 h post induction of encystation. Our data shows
182 that UAE is slightly increased by 1.5 h and G6PI-B began to increase by 4 h (Fig. S2B). At 18 h,
183 UAE, G6PI-B, and GNPNAT levels increased by 150, 20, and 28 fold, respectively (Fig. 2B-C). We
184 next expressed MYB2 and GLP4 CRISPRi guide RNAs individually in G6PI-B, GNPNAT, and UAE
185 NanoLuc cell lines to investigate whether MYB2 and GLP4 modulate their expression.
186 Consistent with our CWP1-2 results, the levels of G6PI-B, UAE, and GNPANT are downregulated
187 in MYB2 knockdown but are upregulated by GLP4 knockdown, suggesting GLP4 is also a
188 repressor of enzymes in the GalNAc pathway (Fig. 3G-I).

189

190 **GLP4 is a cell cycle dependent repressor**

191 Encystation-induced G2 arrest has been demonstrated in *Giardia* (42, 43). Indeed, our data is
192 consistent with previous studies that found 1.5 h of encystation is sufficient to cause
193 accumulation of G2+M cells with a corresponding reduction of cells in G1+S (Fig. 4A-B). A
194 previous study showed that *Giardia* trophozoites arrested at G2 with aphidicolin, produced
195 more ESVs after release into encystation medium (42). This study therefore hypothesized that
196 *Giardia* enter the encystation program at G2. However, evidence to correlate CWP1 and MYB2
197 levels with DNA content during encystation is still lacking. In *Giardia*, nocodazole and
198 aphidicolin treatments or counterflow centrifugal elutriation (CCE) have been used to
199 synchronize trophozoites but there are two technical challenges: (1) Nocodazole and
200 aphidicolin created endoreplication and double-stranded DNA breaks, respectively, and
201 secondary effects resulted in unhealthy cells that would not be ideal for encystation assays
202 (44); (2) the CCE method was performed in 1XHEPES-buffered saline (HBS) and *Giardia*
203 trophozoites are not able to encyst in HBS buffer (44). To more precisely define CWP1 and
204 MYB2 expression levels during encystation at G1 and G2 phases, we analyzed encysting cells
205 with flow cytometry. CWP1 and MYB2 were endogenously tagged with mNG and the cell lines
206 were exposed to encystation stimuli. DNA content was measured by DRAQ5 fluorescence
207 intensity using flow cytometry. A control experiment was performed to verify that the mNG tag
208 does not change CWP1 production in response to encystation stimuli (Fig. S10A-B). We found
209 that cells with higher DNA content had higher CWP1 levels (Fig. S10C). We also used MYB2-
210 mNG to show that G2+M cells have higher MYB2 levels (Fig. S10D), suggesting higher
211 expression of CWP1 was due to higher levels of MYB2. In contrast with the previous conclusion
212 that only G2 cells enter the encystation pathway (42), it is noteworthy that our result indicates
213 that G1 cells produce both CWP1 and MYB2 at 1.5 h post induction of encystation, suggesting
214 *Giardia* enter the encystation program at both G1 and G2 phases instead of G2 only. Given that
215 G2 cells have higher expressions of CWP1 and MYB2, we sought to characterize the expression
216 level of GLP4 in G1 cells. We examined the relationship between GLP4-mNG and the cell cycle
217 at 0 and 1.5 h of encystation. We found that GLP4-mNG fluorescence intensity was increased by
218 1.5 fold in G1+S cells at 1.5 h post induction of encystation but slightly decreased in cells at
219 G2+M (Fig. 4C), suggesting lower GLP4 levels permit G2+M cells to produce more MYB2 and
220 CWP1 during encystation. Because MYB2 and CWP1 levels are lower in G1+S cells, we
221 questioned if GLP4 might be an upstream repressor of MYB2. We transfected the GLP4 CRISPRi
222 guide RNA into the MYB2-NanoLuc expressing cell line. We found that MYB2 levels rose by 1.2
223 fold in the GLP4 knockdown cell line at 4h post inducing encystation, which is consistent with
224 MYB2 ultimately regulating CWP1 levels (Fig. 4D). In contrast, overexpression of GLP4
225 downregulated MYB2 expression by 50% (Fig. 4E-F) and resulted in reduced CWP1 levels (Fig.
226 S8E). These findings suggest MYB2 is downstream of GLP4.

227 Because E2F1 and PAX1 have been shown to upregulate CWP1-3 and MYB2 (26, 29), we sought
228 to determine whether GLP4 modulates MYB2 through either E2F1 or PAX1 expression levels.
229 Interestingly, knockdown of GLP4 did not alter E2F1 or PAX1 expression levels as measured

230 with NanoLuc reporters (Fig. S10F-G), suggesting E2F1 and PAX1 are not downregulated by
231 GLP4. Thus, MYB2 is a downstream of GLP4 but an upstream regulator of CWP1-2 and enzymes
232 in the GalNAc pathway. In summary, GLP4 has a role in limiting entry into the encystation
233 pathway where MYB2 is repressed in G1+S cells by GLP4, then during G2+M, GLP4 levels drop
234 and MYB2 expression is upregulated to produce more CWPs and enzymes in the GalNAc
235 pathway (Fig. 5).

236

237 **Discussion**

238 Previous studies revealed that TFs play important roles in coordinating the late stages of
239 encystation. However, the contribution of TFs during the early stage of encystation was largely
240 unknown. Here we systematically studied the expression profiles of 6 TFs in the early stage of
241 encystation. We utilized CRISPRi- and CasRX-mediated knockdown tools to delineate the role of
242 early upregulated TFs in encystation. We identified GLP4, a previously unstudied TF, as a cell
243 cycle-dependent repressor of early encystation. GARP TFs are commonly considered to be
244 plant-specific, but are also found in protists. Several plant GARP TFs are required for
245 differentiation in *Arabidopsis*, such as reproductive organ determination (44). In our model,
246 encystation stimuli cause *Giardia* trophozoites to accumulate at G2+M phase, and both G1+S
247 and G2+M cells enter the encystation program (Fig. 5). Interestingly, GLP4 expression is rapidly
248 upregulated in the G1+S population to repress MYB2 and CWP1 levels (Fig. 5). In contrast, GLP4
249 levels in the G2+M population is slightly decreased, thus allowing the activation of MYB2 to
250 upregulate the expression of CWP1-2 as well as enzymes in the GalNAc pathway (Fig. 5). This
251 model suggests that a lower dose of GLP4 in G2+M cells permits upregulation of MYB2 and
252 encystation specific genes while a higher dose of GLP4 in G1+S cells downregulates MYB2 and
253 the encystation program.

254 Our observations provide new insights into regulation of stage conversion in *Giardia*. First, our
255 results indicate that GLP4 prevents some cells from encysting and therefore GLP4 has a role in
256 controlling the balance between proliferative growth and terminal differentiation into
257 infectious cysts. It would be interesting to extend our *in vitro* studies into an *in vivo* model of
258 infection to confirm a role for GLP4 in regulating the balance between persistence of infection
259 and transmission. Second, previous studies indicated negative cis-acting regulatory elements
260 are present in CWP2 and G6PI-B promoters (32, 33). We have noticed CWP2 and G6PI-B
261 promoters contain GARP binding sequence (A/G)ATCN (25). Although our results showed that
262 CWP1-2, G6PI-B, UAE, and GNPNAT are upregulated in GLP4 mutants, how this newly identified
263 repressor GLP4 interacts with promoter binding sequence and other TFs is worth further
264 investigation. Third, phospho-regulation may play a key role in regulating entry into the
265 encystation pathway. *Arabidopsis* nucleus-localized GARP TFs, type B ARRs, were activated
266 through a phosphorylation cascade to modulate plant hormone cytokinin signaling (45).
267 *Giardia's* cyclin dependent kinase 2 (CDK2) is upregulated at G2+M (46) and has been shown to
268 activate MYB2 through phosphorylation (47). Two recent RNAseq studies also identified an

269 encystation-upregulated cyclin (GL50803_15532) (13) and G2-dependent TF GLP1
270 (GL50803_7272) (46). In the future, it would be interesting to explore how GLP1, GLP4, CDK2,
271 and cyclin work together to initiate encystation.

272 Our findings advance the understanding of the dynamics of TFs expression in the early phase of
273 encystation in *Giardia*. Moreover, our results demonstrate an unexpected role for the cell cycle-
274 dependent GLP4 transcriptional repressor in regulating MYB2 and the cyst production
275 pathways. The theory of dosage-dependent transcriptional responses is essential for
276 understanding how mammalian and plant cells modulate differentiation (48). Our findings on
277 MYB2 and GLP4 suggests that *Giardia*, a single-celled organism, employs dosage-dependent
278 transcriptional responses to tune the initiation of differentiation.

279

280 # Methods

281 **Giardia growth and encystation media**

282 *Giardia intestinalis* isolate WB clone C6 (ATCC catalog number 50803; American Type culture collection)
283 were cultured in TYDK media at pH 7.1 supplemented with 10% adult bovine serum and 0.125 mg/ml
284 bovine bile(49). To induce encystation, cells were cultured 48 h in pH 6.8 pre-encystation media without
285 bile then one of three encystation protocols were used: (1) Uppsala encystation protocol: TYDK media at
286 pH 7.8 supplemented with 10% adult bovine serum and 5 mg/ml bovine bile(14); (2) Two-step protocol:
287 TYDK media at pH 7.8 supplemented with 10% adult bovine serum, 0.25 mg/ml porcine bile and 5 mM
288 lactic acid(50); (3) Lipoprotein-deficient protocol: TYDK media at pH 7.8 supplemented with lipoprotein-
289 deficient serum(40).

290 **Plasmid construction**

291 **mNeonGreen and NanoLuc fusions**

292 Coding sequences were PCR-amplified from *Giardia lamblia* genomic DNA. Primers sequences are
293 indicated in the supplemental excel file Table S1. The mNeonGreen and NanoLuc vectors were digested
294 with the indicated restriction enzymes and a PCR amplicon was ligated using Gibson assembly(51). The
295 resulting constructs were linearized with the restriction enzyme indicated in supplemental Table S1
296 before electroporation for integration into the endogenous locus(52). Neomycin and puromycin were
297 used for selection.

298 **CasRX expression cassette design**

299 EsCas13d (Catalog #108303), CasRX (Cat #109049), and PspCas13b (Cat#103862) were obtained from
300 Addgene. Cas 13 fragments were PCR amplified, digested with restriction enzymes and inserted into
301 pPAC-3HA expression cassettes under the GDH promoter(53). The Cas13-3HA expression vectors were
302 linearized with SwaI and electroporated into *Giardia lamblia* so that expression levels could be
303 monitored by western blotting. To generate the CasRX expression system, the CRISPRi expression vector
304 (dCas9g1pac) was used as a backbone and dCas9 was replaced with CasRX and the gRNA scaffold
305 sequence (SCF) was replaced with the CasRX-specific direct repeat (DR) (37).

306 **Design of guide RNA**

307 Guide RNA for the CRISPRi system utilized the Dawson Lab protocol (34), NGG PAM sequence and G.
308 Lamblia ATCC 50803 genome were selected for CRISPRi guide RNA design with Benchling. Cas13 guide
309 RNA designs were based on the Sanjana Lab Cas13 guide tool (https://cas13design.nygenome.org/)(54).

310 **In vitro bioluminenscence assays**

311 *Giardia* cells were iced for 15 min and centrifuged at 700 x g for 7 min at 4°C. Cells were resuspended in
312 cold 1X HBS (HEPES-buffered saline) and serial dilutions were made after counting cells with a MOXI Z
313 mini Automated Cell Counter Kit (Orflo, Kenchum, ID). To measure NanoLuc luminescence, 20,000 cells
314 were loaded into white polystyrene, flat bottom 96-well plates (Corning Incorporated, Kennebunk, ME)
315 then mixed with 10 μl of NanoGlo luciferase assay reagent (Promega). Relative luminescence units (RLU)
316 were detected on a pre-warmed 37°C EnVision plate reader (Perkin Elmer, Waltham, MA) for 30 min to
317 reach the maximum value. Experiments are from three independent bioreplicates. To measure CBG99
318 luminescence, 20,000 cells were loaded into white polystyrene, flat bottom 96-well plates then mixed
319 with 50 μl of 10 mg/mL D-luciferin. Relative luminescence units (RLU) were detected as above.

320 **Protein blotting**

321 *Giardia* parasites were iced for 30 min then centrifuged at 700 x g for 7 min and washed twice in 1X HBS
322 supplemented with HALT protease inhibitor (Pierce) and phenylmethylsulfonyl fluoride (PMSF). The cells
323 were resuspended in 300 μl of lysis buffer containing 50 mM Tris-HCl pH 7.5, 150 mM NaCl, 7.5%
324 glycerol, 0.25 mM $CaCl_2$, 0.25 mM ATP, 0.5 mM Dithiotheitol, 0.5 mM PMSF (Phenylmethylsulfonyl
325 flroride), 0.1% Trition X-100 and Halt protease inhibitors (Pierce). The sample was pelleted at 700 x g for
326 7 min, the resulting supernatant was mixed with 2X sample buffer (Bio-Rad) and boiled at 98°C for 5
327 min. Protein samples were separated using sodium dodecyl sulfate (SDS) polyacrylamide gel
328 electrophoresis. Protein transfer was performed using an Immobilon-FL membrane (Millipore). To
329 detect tubulin, a mouse monoclonal anti-acetylated tubulin clone 6-11B-1 antibody (IgG2b; product T
330 6793; Sigma-Aldrich) were used at 1:2,500 dilution and secondary anti-mouse isotype-specific antibody
331 conjugated with Alexa 488 (anti-IgG2b) were used at 1:2,500. To detect CWP1, Alexa 647-conjugated
332 anti-CWP1 antibody (Waterborne, New Orleans, LA) was used at 1:2,000. Multiplex immunoblots were
333 imaged using a Chemidoc MP system (Bio-Rad).

334 **Immunofluorescence**

335 *Gairdia* parasites were iced for 30 min and pelleted at 700 x g for 7 min. The pellet was fixed in PME
336 buffer (100 mM Piperazine-N,N'-bis (ethanesulfonic acid) (PIPES) pH 7.0, 5 mM EGTA, 10 mM $MgSO_4$
337 supplemented with 1% paraformaldehyde (PFA) (Electron Microscopy Sciences, Hatfield, PA), 100 μM 3-
338 maleimidobenzoic acid N-hydroxysuccinimide ester (Sigma-Aldrich), 100 μM ethylene glycol bis
339 (succinimidyl succinate) (Pierce), and 0.025% Triton X-100 for 30 min at 37°C. Fixed cells were attached
340 to polylysine coated coverslips. Cells were washed once in PME and permeabilized with PME plus 0.1%
341 Triton X-100 for 10 min. After two quick washes with PME, blocking was performed in PME
342 supplemented with 1% bovine serum albumin, 0.1% NaN_3, 100 mM lysine, 0.5% cold water fish skin
343 gelatin (Sigma-Aldrich). Next, 1:200 diluted Alexa 647-conjugated anti-CWP1 antibody (Waterborne,
344 New Orleans, LA) was added to incubate for 1 h. Cells were washed three times in PME plus 0.05%
345 Triton X-100. Coverslips were mounted with ProLong Gold antifade plus 4',6-diamidino-2-phenylinodole

346 (DAPI; Molecular Probes). Images were acquired on a DeltaVision Elite microscope using a 60X, 1.4-
347 numerical aperture objective with a PCO Edge sCMOS camera, and images were deconvolved using
348 SoftWorx (API, Issaquah, WA).

349 **Imaging and image analysis**

350 Analyses of CWP1-stained vesicle size and number were performed with Imaris software (Bitplane,
351 version 8.1). ImageJ was used to process all images and figures were assembled using Adobe Illustrator.

352 **Cyst count and cyst viability staining**

353 To collect water-resistant *Giardia* cysts, confluent *Giardia* trophozoites were incubated in encystation
354 media supplemented with 10 g/L ovine bovine bile and calcium lactate. To count cyst, 20 µl of 48 h
355 encysted cells were counted using a hemocytometer. To determine cyst viability, 48 h encysted *Giardia*
356 cells were centrifuged at 700 x g for 7 min and the pellets were washed 10 times in deionized water,
357 then stored in distill water overnight at 4°C. The next day, fluorescein diacetate (FDA) and propidium
358 iodide (PI) were used to stain live and dead cysts, respectively, and images were collected using a
359 DeltaVision Elite microscope with a 40X, 1.4-numerical apeture objective with a PCO Edge sCMOS
360 camera, and images were deconvolved using SoftWorx (API, Issaquah, WA).

361 **Flow cytometry assay**

362 Flow cytometry analysis was performed after fixation with 0.25% PFA at 4°C for 15 min. 1 µM DRAQ5
363 (Thermo Scientific Cat# 62251) was used to stain DNA. 10,000 cells per sample were analyzed using a
364 FACS Canto II Flow Cytometer at the Pathology Flow Cytometry Core Facility (Department of Pathology,
365 University of Washington). Data were analyzed using FlowJo.

366

367 **Acknowledgements**

368 We thank Paredez laboratory undergraduate students Bailin Zhang, Greyson Hamilton, and
369 Daria Rydell and our colleagues at UW Biology for discussions and comments on the
370 manuscripts, and Xiao Ping from the flow cytometry facility at UW Pathology. We thank Photini
371 Sinnis, Kirk Deitsch, Patricia Johnson for inviting us to participate in the 40th-Biology of
372 Parasitism (BoP) course where BoP students helped to initiate this project. We thank Dr. Scott
373 Dawson for gifting us the CRISPRi plasmid and Dr. Barbara Wakimoto and Dr. Melissa Steele-
374 Ogus for providing comments on the manuscript. Research was funded by University of
375 Washington Bridge funds and NIAD 1R21AI159035 to ARP.

376

377

378 1. P. Schaap, C. Schilde, Encystation: the most prevalent and underinvestigated differentiation
379 pathway of eukaryotes. *Microbiology (Reading, England)* **164**, 727-739 (2018).
380 2. Y. Fakhri *et al.*, The risk factors for intestinal Giardia spp infection: Global systematic review and
381 meta-analysis and meta-regression. *Acta tropica* 10.1016/j.actatropica.2021.105968, 105968
382 (2021).

383 3. A. Waldram, R. Vivancos, C. Hartley, K. Lamden, Prevalence of Giardia infection in households of
384 Giardia cases and risk factors for household transmission. *BMC infectious diseases* **17**, 486
385 (2017).
386 4. S. G. Wright, Protozoan infections of the gastrointestinal tract. *Infectious disease clinics of North*
387 *America* **26**, 323-339 (2012).
388 5. R. Argüello-Garciá, M. L. Bazán-Tejeda, G. Ortega-Pierres, Encystation commitment in Giardia
389 duodenalis: a long and winding road. *Parasite (Paris, France)* **16**, 247-258 (2009).
390 6. T. Lauwaet, B. J. Davids, D. S. Reiner, F. D. Gillin, Encystation of Giardia lamblia: a model for
391 other parasites. *Current opinion in microbiology* **10**, 554-559 (2007).
392 7. H. D. Luján, M. R. Mowatt, L. G. Byrd, T. E. Nash, Cholesterol starvation induces differentiation of
393 the intestinal parasite Giardia lamblia. *Proceedings of the National Academy of Sciences* **93**,
394 7628-7633 (1996).
395 8. N. R. Barash *et al.*, Giardia Colonizes and Encysts in High-Density Foci in the Murine Small
396 Intestine. *mSphere* **2** (2017).
397 9. C. Faso, A. B. Hehl, Membrane trafficking and organelle biogenesis in Giardia lamblia: use it or
398 lose it. *Int J Parasitol* **41**, 471-480 (2011).
399 10. K. Sener, Z. Shen, D. S. Newburg, E. L. Jarroll, Amino sugar phosphate levels in Giardia change
400 during cyst wall formation. *Microbiology (Reading, England)* **150**, 1225-1230 (2004).
401 11. E. L. Jarroll *et al.*, Regulation of carbohydrate metabolism during Giardia encystment. *The*
402 *Journal of eukaryotic microbiology* **48**, 22-26 (2001).
403 12. E. L. Jarroll, P. Manning, D. G. Lindmark, J. R. Coggins, S. L. Erlandsen, Giardia cyst wall-specific
404 carbohydrate: evidence for the presence of galactosamine. *Molecular and biochemical*
405 *parasitology* **32**, 121-131 (1989).
406 13. L. Rojas-López *et al.*, A Detailed Gene Expression Map of Giardia Encystation. *Genes* **12** (2021).
407 14. E. Einarsson *et al.*, Coordinated Changes in Gene Expression Throughout Encystation of Giardia
408 intestinalis. *PLOS Neglected Tropical Diseases* **10**, e0004571 (2016).
409 15. J. K. Pham *et al.*, Transcriptomic Profiling of High-Density Giardia Foci Encysting in the Murine
410 Proximal Intestine. *Frontiers in cellular and infection microbiology* **7**, 227 (2017).
411 16. R. Bernander, J. E. Palm, S. G. Svard, Genome ploidy in different stages of the Giardia lamblia life
412 cycle. *Cell Microbiol* **3**, 55-62 (2001).
413 17. T. J. Byers, B. G. Kim, L. E. King, E. R. Hugo, Molecular aspects of the cell cycle and encystment of
414 Acanthamoeba. *Reviews of infectious diseases* **13 Suppl 5**, S373-384 (1991).
415 18. D. Eichinger, Encystation of entamoeba parasites. *BioEssays : news and reviews in molecular,*
416 *cellular and developmental biology* **19**, 633-639 (1997).
417 19. S. G. Svärd, P. Hagblom, J. E. D. Palm, Giardia lamblia — a model organism for eukaryotic cell
418 differentiation. *FEMS Microbiology Letters* **218**, 3-7 (2003).
419 20. B. S. Waldman *et al.*, Identification of a Master Regulator of Differentiation in Toxoplasma. *Cell*
420 **180**, 359-372.e316 (2020).
421 21. C.-H. Sun, D. Palm, A. G. McArthur, S. G. Svärd, F. D. Gillin, A novel Myb-related protein involved
422 in transcriptional activation of encystation genes in Giardia lamblia. *Molecular Microbiology* **46**,
423 971-984 (2002).
424 22. G. M. Ehrenkaufer, J. A. Hackney, U. Singh, A developmentally regulated Myb domain protein
425 regulates expression of a subset of stage-specific genes in Entamoeba histolytica. *Cellular*
426 *microbiology* **11**, 898-910 (2009).
427 23. C. Faso, S. Bischof, A. B. Hehl, The proteome landscape of Giardia lamblia encystation. *PLoS One*
428 **8**, e83207 (2013).
429 24. J. K. Pham *et al.*, Transcriptomic Profiling of High-Density Giardia Foci Encysting in the Murine
430 Proximal Intestine. *Frontiers in cellular and infection microbiology* **7** (2017).

431 25. C. H. Sun, L. H. Su, F. D. Gillin, Novel plant-GARP-like transcription factors in Giardia lamblia.
432 *Molecular and biochemical parasitology* **146**, 45-57 (2006).
433 26. L.-H. Su *et al.*, A Novel E2F-like Protein Involved in Transcriptional Activation of Cyst Wall Protein
434 Genes in Giardia lamblia*. *Journal of Biological Chemistry* **286**, 34101-34120 (2011).
435 27. Y. J. Pan, C. C. Cho, Y. Y. Kao, C. H. Sun, A novel WRKY-like protein involved in transcriptional
436 activation of cyst wall protein genes in Giardia lamblia. *The Journal of biological chemistry* **284**,
437 17975-17988 (2009).
438 28. S.-F. Chuang, L.-H. Su, C.-C. Cho, Y.-J. Pan, C.-H. Sun, Functional Redundancy of Two Pax-Like
439 Proteins in Transcriptional Activation of Cyst Wall Protein Genes in Giardia lamblia. *PLOS ONE* **7**,
440 e30614 (2012).
441 29. Y.-T. Wang *et al.*, A novel pax-like protein involved in transcriptional activation of cyst wall
442 protein genes in Giardia lamblia. *J Biol Chem* **285**, 32213-32226 (2010).
443 30. C. H. Wang, L. H. Su, C. H. Sun, A novel ARID/Bright-like protein involved in transcriptional
444 activation of cyst wall protein 1 gene in Giardia lamblia. *The Journal of biological chemistry* **282**,
445 8905-8914 (2007).
446 31. L. Morf *et al.*, The transcriptional response to encystation stimuli in Giardia lamblia is restricted
447 to a small set of genes. *Eukaryot Cell* **9**, 1566-1576 (2010).
448 32. S. R. Davis-Hayman, J. R. Hayman, T. E. Nash, Encystation-specific regulation of the cyst wall
449 protein 2 gene in Giardia lamblia by multiple cis-acting elements. *International journal for*
450 *parasitology* **33**, 1005-1012 (2003).
451 33. L. A. Knodler, S. G. Svärd, J. D. Silberman, B. J. Davids, F. D. Gillin, Developmental gene regulation
452 in Giardia lamblia: first evidence for an encystation-specific promoter and differential 5' mRNA
453 processing. *Molecular microbiology* **34**, 327-340 (1999).
454 34. S. G. McInally *et al.*, Robust and stable transcriptional repression in Giardia using CRISPRi. *Mol*
455 *Biol Cell* **30**, 119-130 (2019).
456 35. A. E. Masser, G. Kandasamy, J. M. Kaimal, C. Andréasson, Luciferase NanoLuc as a reporter for
457 gene expression and protein levels in Saccharomyces cerevisiae. *Yeast (Chichester, England)* **33**,
458 191-200 (2016).
459 36. C. G. England, E. B. Ehlerding, W. Cai, NanoLuc: A Small Luciferase Is Brightening Up the Field of
460 Bioluminescence. *Bioconjugate chemistry* **27**, 1175-1187 (2016).
461 37. S. Konermann *et al.*, Transcriptome Engineering with RNA-Targeting Type VI-D CRISPR Effectors.
462 *Cell* **173**, 665-676.e614 (2018).
463 38. Y.-C. Huang *et al.*, Regulation of Cyst Wall Protein Promoters by Myb2 in Giardia lamblia*.
464 *Journal of Biological Chemistry* **283**, 31021-31029 (2008).
465 39. S. A. Michaels *et al.*, Methionyl-tRNA synthetase inhibitor has potent in vivo activity in a novel
466 Giardia lamblia luciferase murine infection model. *The Journal of antimicrobial chemotherapy*
467 **75**, 1218-1227 (2020).
468 40. H. D. Luján, M. R. Mowatt, L. G. Byrd, T. E. Nash, Cholesterol starvation induces differentiation of
469 the intestinal parasite Giardia lamblia. *Proceedings of the National Academy of Sciences of the*
470 *United States of America* **93**, 7628-7633 (1996).
471 41. C. H. Sun, D. Palm, A. G. McArthur, S. G. Svärd, F. D. Gillin, A novel Myb-related protein involved
472 in transcriptional activation of encystation genes in Giardia lamblia. *Molecular microbiology* **46**,
473 971-984 (2002).
474 42. D. S. Reiner *et al.*, Synchronisation of Giardia lamblia: identification of cell cycle stage-specific
475 genes and a differentiation restriction point. *Int J Parasitol* **38**, 935-944 (2008).
476 43. S. C. Dawson, E. Nohýnková, M. Cipriano, "Cell Cycle Regulation and Cell Division in Giardia" in
477 Giardia: A Model Organism, H. D. Luján, S. Svärd, Eds. (Springer Vienna, Vienna, 2011),
478 10.1007/978-3-7091-0198-8_10, pp. 161-183.

44. A. Safi *et al.*, The world according to GARP transcription factors. *Current opinion in plant biology* **39**, 159-167 (2017).
45. J. Kim, Phosphorylation of A-Type ARR to function as negative regulator of cytokinin signal transduction. *Plant signaling & behavior* **3**, 348-350 (2008).
46. J. Kim, M. Y. Shin, S.-J. Park, RNA-sequencing Profiles of Cell Cycle?Related Genes Upregulated during the G2-Phase in Giardia lamblia. *Korean J Parasitol* **57**, 185-189 (2019).
47. C. C. Cho, L. H. Su, Y. C. Huang, Y. J. Pan, C. H. Sun, Regulation of a Myb transcription factor by cyclin-dependent kinase 2 in Giardia lamblia. *The Journal of biological chemistry* **287**, 3733-3750 (2012).
48. H. F. Hofhuis, R. Heidstra, Transcription factor dosage: more or less sufficient for growth. *Current opinion in plant biology* **45**, 50-58 (2018).
49. D. B. Keister, Axenic culture of Giardia lamblia in TYI-S-33 medium supplemented with bile. *Transactions of the Royal Society of Tropical Medicine and Hygiene* **77**, 487-488 (1983).
50. F. D. Gillin, S. E. Boucher, S. S. Rossi, D. S. Reiner, Giardia lamblia: the roles of bile, lactic acid, and pH in the completion of the life cycle in vitro. *Experimental parasitology* **69**, 164-174 (1989).
51. D. G. Gibson *et al.*, Enzymatic assembly of DNA molecules up to several hundred kilobases. *Nature Methods* **6**, 343-345 (2009).
52. S. Gourguechon, L. J. Holt, W. Z. Cande, The Giardia cell cycle progresses independently of the anaphase-promoting complex. *Journal of cell science* **126**, 2246-2255 (2013).
53. S. Gourguechon, W. Z. Cande, Rapid tagging and integration of genes in Giardia intestinalis. *Eukaryot Cell* **10**, 142-145 (2011).
54. H. H. Wessels *et al.*, Massively parallel Cas13 screens reveal principles for guide RNA design. *Nature biotechnology* **38**, 722-727 (2020).
55. D. B. T. Cox *et al.*, RNA editing with CRISPR-Cas13. *Science (New York, N.Y.)* **358**, 1019-1027 (2017).

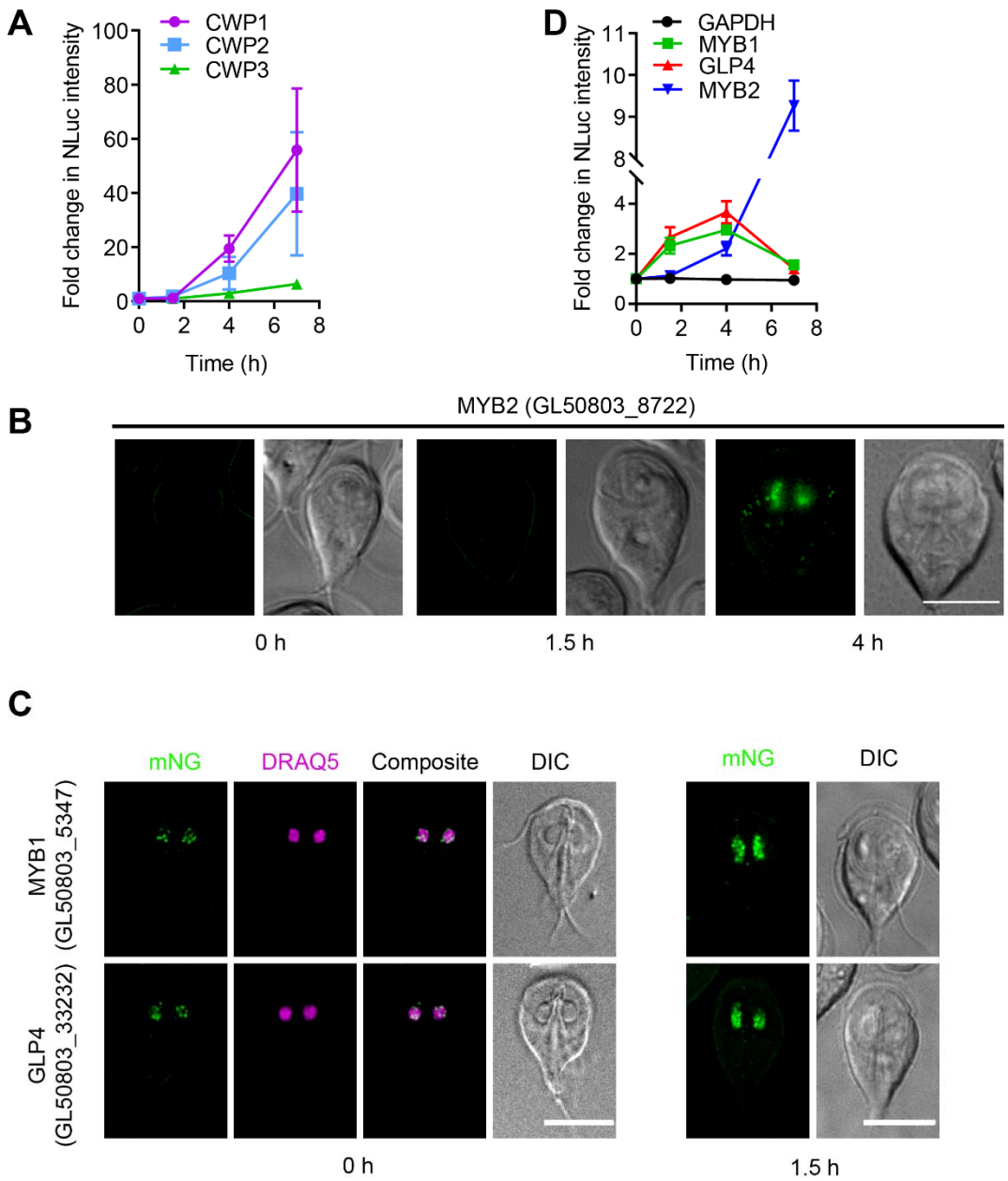

Fig. 1. GLP4 and MYB1 are rapidly upregulated TFs. *(A)* Relative NanoLuc (NLuc) luciferase intensity of endogenously tagged CWP1-NLuc, CWP2-NLuc, and CWP3-NLuc after 0, 1.5, and 4 h exposure to encystation medium. The expression level for each time point has three biological replicates. Fold change is normalized to 0 h. Luciferase intensity is measured by plate reader. Each well has 2 x10^5 cells. *(B)* Nuclear localizations of MYB2-mNG (GL50803_8722), (C) MYB1-mNG (GL50803_5347) and GLP4-mNG (GL50803_33232) after 0, 1.5, 4, and 7 h exposure to encystation medium. MYB1-mNG and GLP4-mNG were colocalized with nuclear DRAQ5 to show nuclear localization at 0 h post induction of encystation. All images were taken with same exposure. Bars, 10 µm. *(D)* Same quantification as (A) with GLP4-NLuc, MYB1-NLuc, MYB2-NLuc, and GAPDH-NLuc after 0, 1.5, 4, 7h exposure to encystation medium.

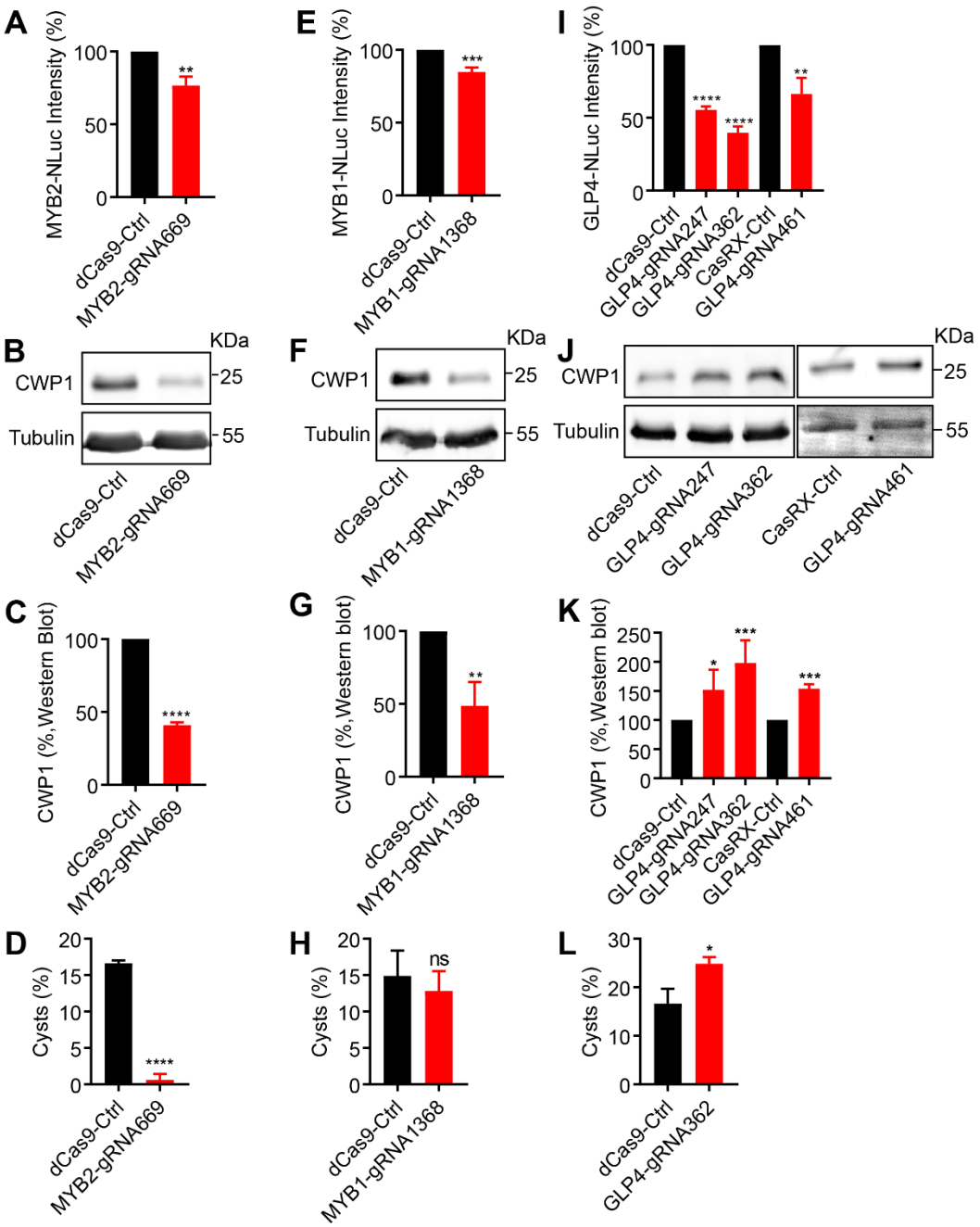

Fig. 2. Depletion of GLP4 increases CWP1 expression level and cyst number. *(A,E,I)* Quantification of NanoLuc intensity from CRISPRi or CasRX-mediated knockdowns of (A) MYB2 (GL50803_8722), (E) MYB1 (GL50803_5347), and (I) GLP4 (GL50803_33232). The expression level is normalized to the dCas9 control. *(B,F,J)* Western blots of CWP1 and tubulin from (B) MYB2, (F) MYB1, (J) GLP4 knockdowns at 4h post induction of encystation. *(C,G,K)* Quantification of Western blots of CWP1 and tubulin from (B) MYB2, (F) MYB1, (J) GLP4. The expression level is normalized to tubulin. *(D,H,L)* Quantification of cyst number for (D) MYB2, (H) MYB1, and (L) GLP4 knockdowns after 48 h encystation quantified by hemocytometer. All quantification is from three independent biological replicates. Data are mean ± s.d. (n>100,000 cysts analyzed) Student's t-test, *p<0.01, **p<0.001, ***p<0.0001, ****p<0.00001, ns= not significant.

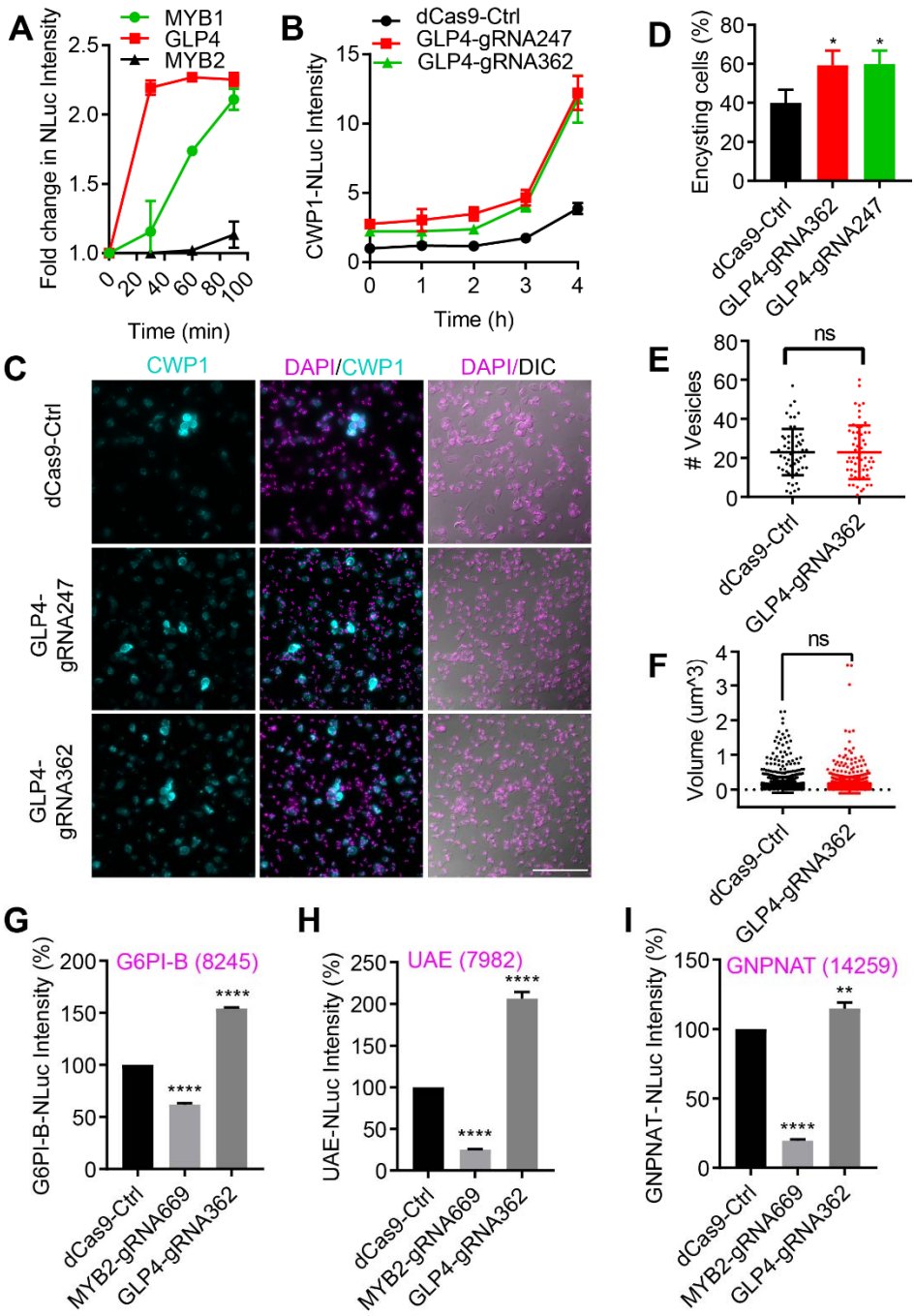

Fig. 3. GLP4 downregulates encystation markers. *(A)* Relative NanoLuc intensity of MYB1-NLuc, MYB2-NLuc, and GARP4-NLuc after 0, 0.5, 1 and 2 h exposure to encystation medium (Uppsala medium). The expression level from each time point has three biological replicates. The fold change is normalized to 0 h. *(B)* Relative CWP1-NLuc intensity in GLP4 knockdown cells after 0, 0.5, 1,2,3 and 4 h exposure to encystation medium (Uppsala medium). The expression level from each time point has three biological replicates. The fold change is normalized to 0 h of the dCas9-Ctrl. *(C)* CWP1 and DAPI staining at 24 h of encystation for dCas9-Ctrl, GLP4-gRNA247, and GLP4-gRNA362 cell lines. Bars, 100 µm. *(D)* Quantification of (C). Data are mean ± s.d. from three independent experiments (total cells counted for dCas9-Ctrl n=1830, GLP4-gRNA362 n=1747, GLP4-gRNA247 n=1783) Student's t-test, *p<0.01. IMARIS-assisted analysis of *(E)* vesicle number and *(F)* vesicle volume in 4 h encysting cells of dCas9-Ctrl, GLP4-gRNA247 and GLP4-gRNA362 cell lines. n.s.= not significant. n=63 cells for dCas9-Ctrl. n= 93 for GLP4-gRNA362. *(G-I)* Relative expression levels of GalNAc enzymes for (G) G6PI-B-NLuc (GL50803_8245), (H) UAE-NLuc (GL50803_7982), and (I) GNPNAT-NLuc (GL50803_14259) in dCas9 control, MYB2-gRNA669, and GLP4-gRNA362 backgrounds. **p<0.001, ****p<0.00001.

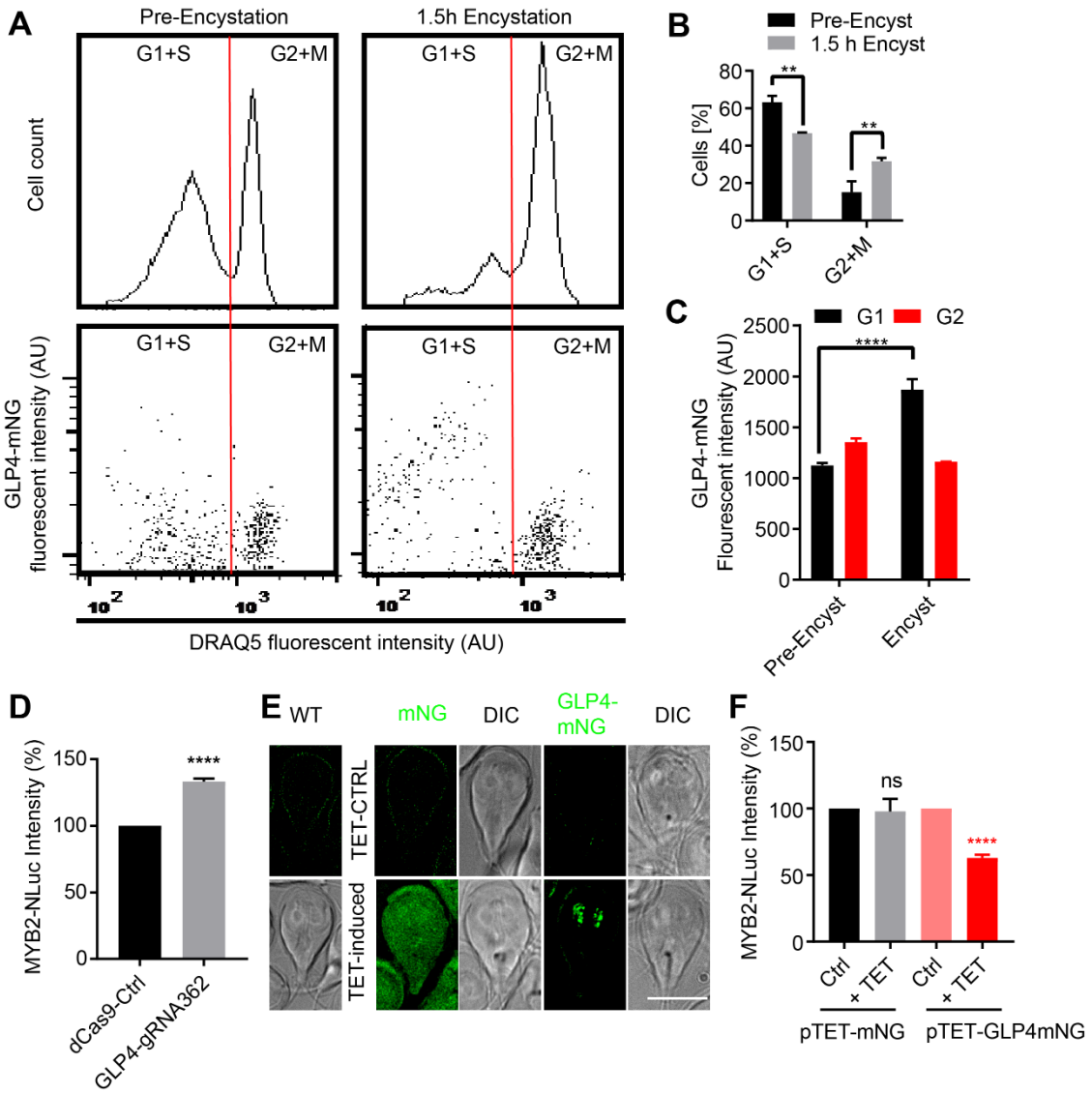

Fig. 4. GLP4 is a cell cycle dependent repressor. *(A)* Flow cytometry analysis of DRAQ5 and GLP4-mNG at 0 and 1.5 h of encystation. Red line is the separation point between G1+S and G2+M phases. *(B)* Quantification of G1+S and G2+M cells from 0 and 1.5 h encystation in (A). Data are mean ± s.d. (n=3, 10,000 cells per replicate) Student's t-test, **p<0.001. *(C)* Quantification of GLP4-mNG fluorescence intensity in G1+S and G2+M cells at 0 and 1.5 h of encystation. Data are mean ± s.d. (n=3) Student's t-test, ****p<0.0001. *(D)* Relative NanoLuc intensity of MYB2 from dCas9 control and GLP4-gRNA362 cell lines. ****p<0.00001. *(E)* Green fluorescence and DIC images of WT, GLP4-mNG (Int) (integrated and endogenously tagged GLP4-mNG), *p*TET-mNG (mNG under the tetracycline inducible promoter) and *p*TET-GLP4-mNG (GLP4-mNG under the tetracycline inducible promoter) in the MYB2-NLuc background with or without tetracycline induction. All images were taken with same exposure. Bars, 10 µm. *(F)* Relative expressions of MYB2-NLuc intensity in mNG and GLP4-mNG overexpression cell lines after 4 h of encystation. Expression levels are normalized to the tetracycline controls at 4 h post induction of encystation. ****p<0.00001. 20 µg/ml tetracycline (final concentration) was added to induce expression for 24 h. ****p<0.00001. n.s.= not significant.

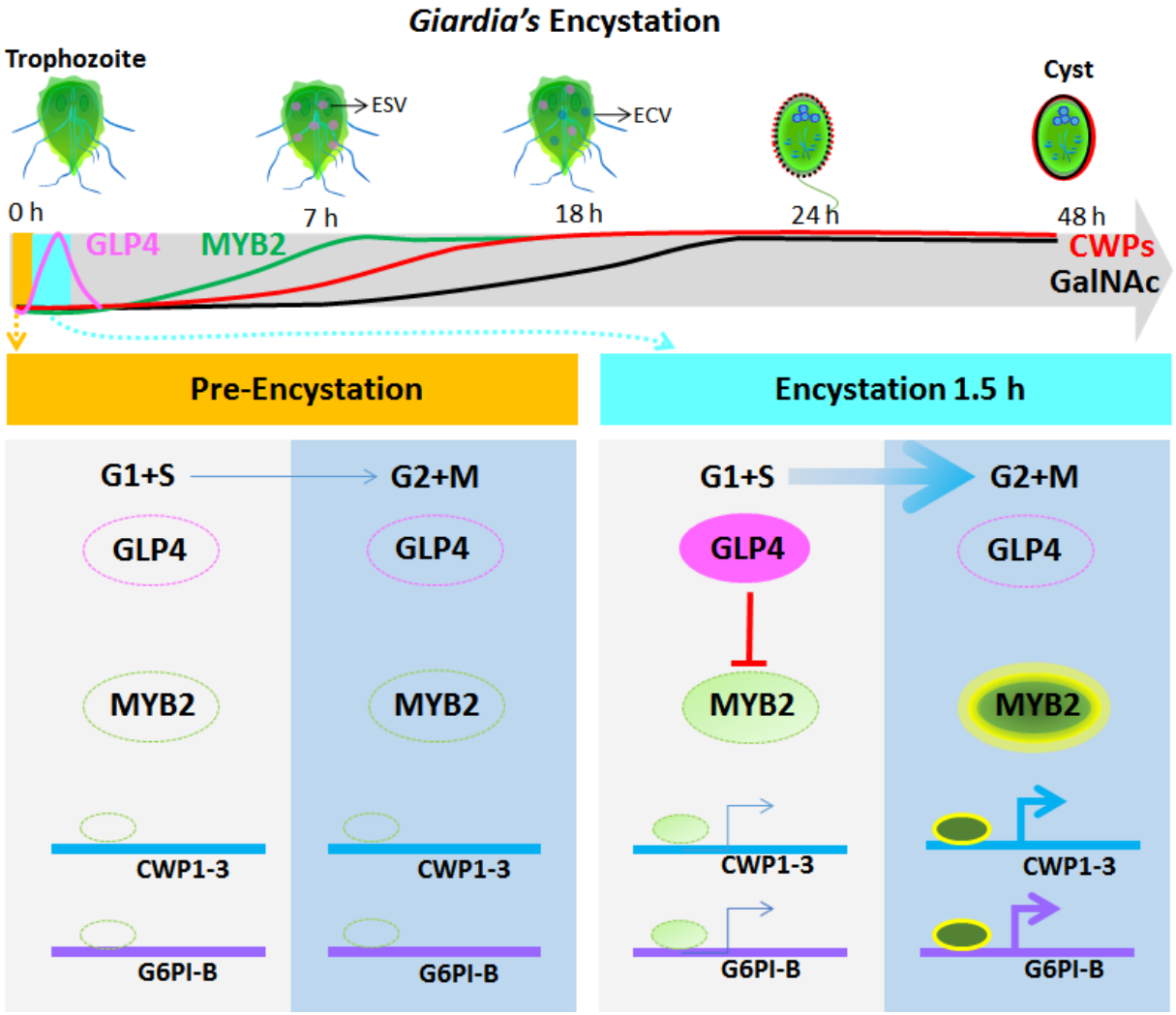

Fig. 5. Schematic overview of the dosage dependent transcriptional responses during encystation. ***Top panel*** shows a timeline for encystation that includes 7 h marked by encystation specific vesicles (ESVs, closed pink circle) that traffic CWPs, the 18 h middle stage with ESVs and the encystation carbohydrate-specific vesicles (ECVs, closed blue circle) that traffic the GalNac sugars, the 24 h middle-late stage with cysts that have begun disassembly of their cytoskeletons, and the 48 h late stage with mature cysts. ***Middle panel*** shows the expression profiles of GLP4 (magenta), MYB2 (green), CWPs (red), and GalNAc enzymes (black) in response to encystation stimuli. GLP4 increases rapidly within 30 min and decreases at 4 h, MYB2 increases at 2-4h, CWPs increase at 2-4h, and enzymes in the GalNAc pathway increase by 7-18 h. ***Bottom panel*** shows the regulatory relationship of GLP4, MYB2, CWPs, and enzymes of the GalNac pathway in G1+S and G2+M cells after exposure to encystation stimuli. Bottom left indicates that GLP4 and MYB2 are not upregulated in the trophozoite (Pre-encystation). CWPs and GalNAc enzymes remain uninduced. Bottom right indicates that *Giardia* cells accumulate in G2+M phase in response to encystation stimuli (accumulation depicted by size of the blue arrows). MYB2 has been shown to bind the promoter regions of CWP1-3 and G6PI-B as well as function as an activator in previous studies. In G1+S phase, GLP4 is upregulated to repress MYB2, hence CWPs and GalNAc enzymes are downregulated. In G2+M phase, GLP4 is downregulated and MYB2 is upregulated. Therefore, CWPs and GalNAc enzymes are upregulated.

603

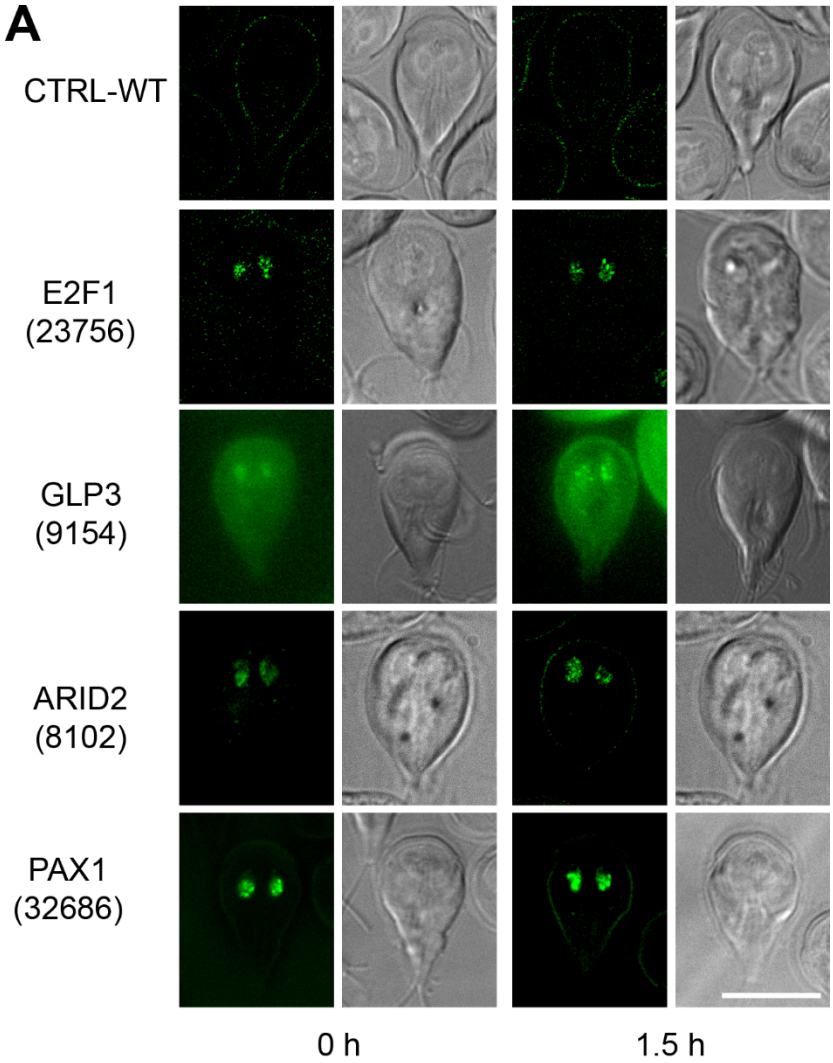

604 **Fig. S1.** Localizations of encystation-induced genes. mNG and DIC images of Wild Type (untagged control
605 cell), and mNG-tagged proteins at the endogenous locus: E2F1 (GL50803_23756), GLP3 (GL50803_9154),
606 ARID2 (GL50803_8102), PAX1 (GL50803_32686) after 0 and 1.5 h exposure to encystation medium. Bars,
607 10 µm.

608

609

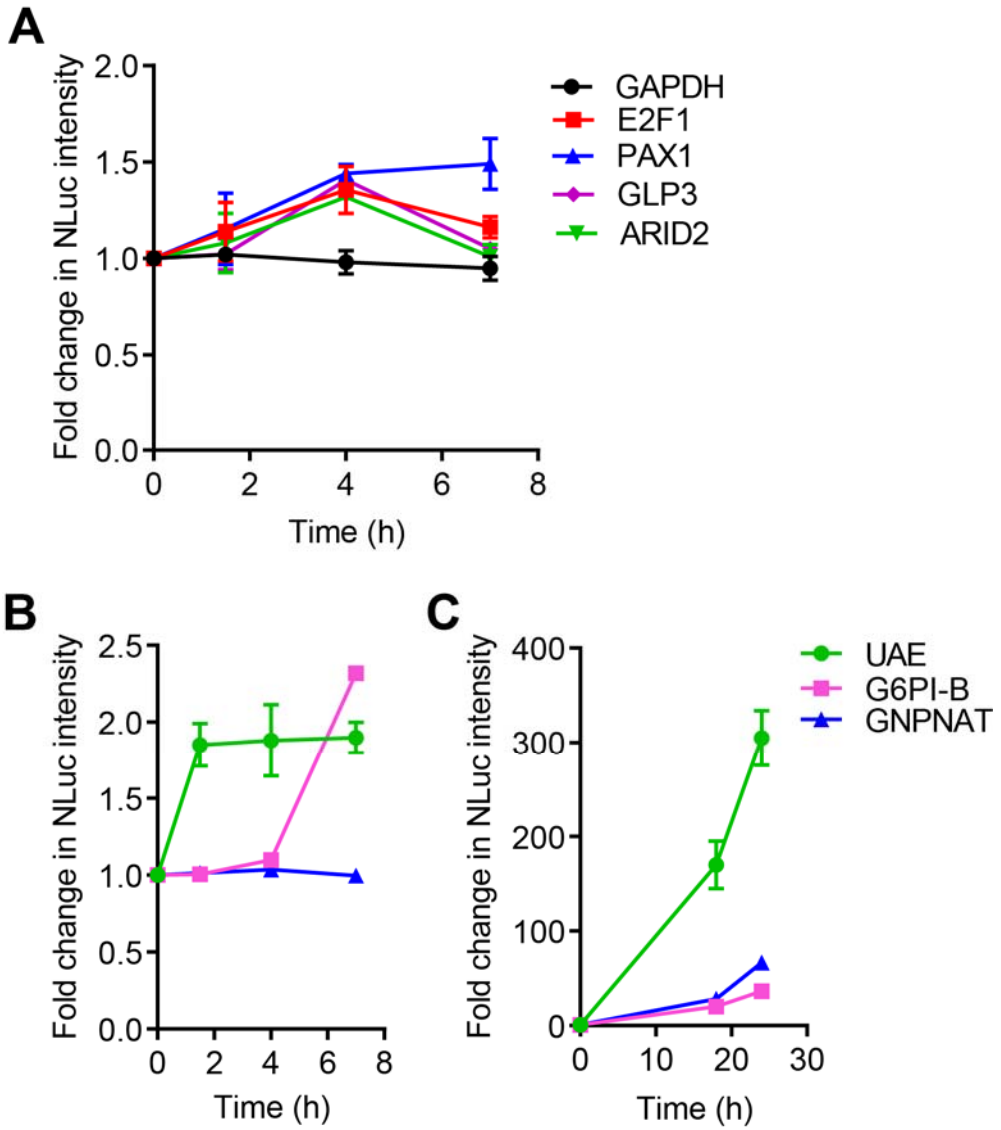

610 **Fig. S2.** E2F1, PAX1, GLP3, and ARID2 are upregulated at 4h. *(A)* Relative expression of NanoLuc intensity
611 for E2F1-NLuc, PAX1-NLuc, ARID2-NLuc, GLP3-NLuc, and GAPDH-NLuc after 0, 1.5, 4, and 7 h exposure to
612 encystation medium. The expression level from each time point has three biological replicates. The fold
613 change is normalized to the 0 h control. *(B-C)* G6PI-B (GL50803_8245), UAE (GL50803_7982), and
614 GNPNAT (GL50803_14259) are upregulated in response to encystation stimuli. Relative NanoLuc
615 intensity of G6PI-B, UAE, and GNPNAT were measured after 0, 1.5, 4, 7, 18, and 24 h exposure to
616 encystation medium. The expression level from each time point has three biological replicates. The fold
617 change is normalized to 0 h.

618

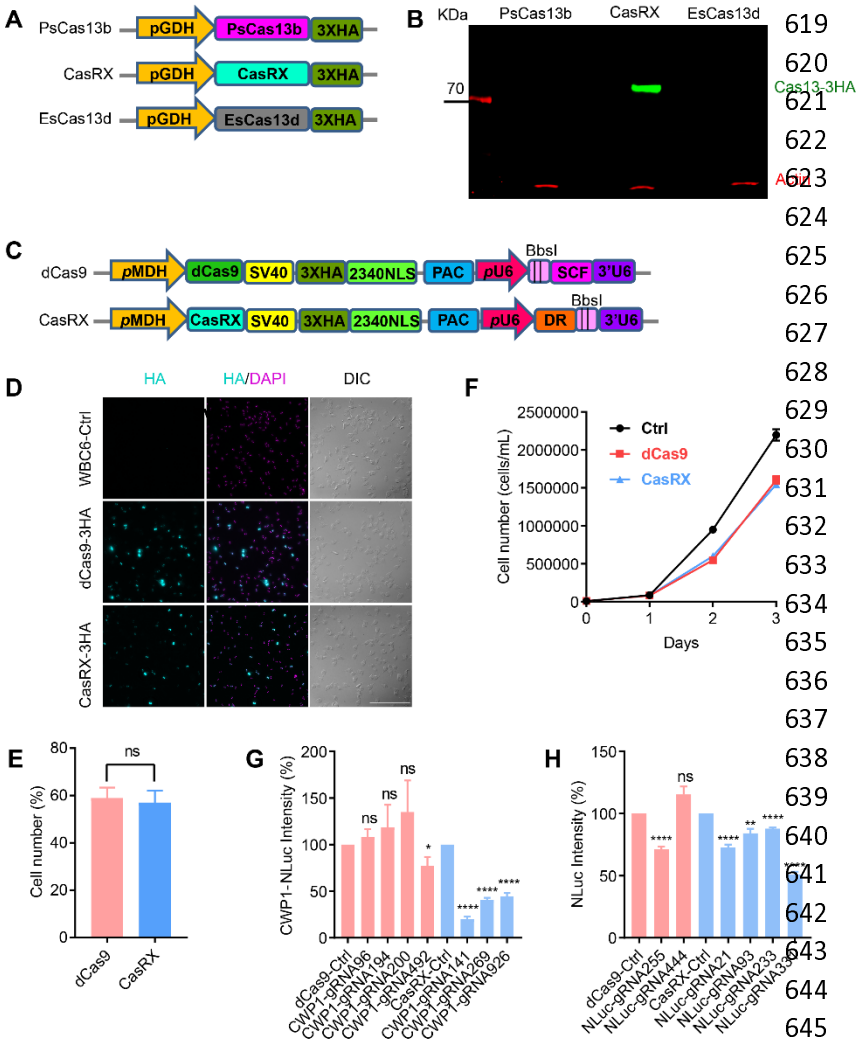

Fig. S3. Development of CasRX for use in *Giardia*. Cas13 enzymes are RNA-targeting CRISPR enzymes which have been shown to have high efficiency and specificity in human cells (37). We first tested the ability to express three Cas13 enzymes, including PsCas13b (55), CasRX (37) and EsCas13d (37). CasRX was the only Cas13 enzyme with good expression in *Giardia*. Starting with the existing CRISPRi vector, we replaced dCas9 and the gRNA scaffold sequence (SCF) with CasRX and the CasRX-specific direct repeat (DR), to establish a functional CasRX knockdown system. *(A,B)* Heterologous expression of 3HA tagged PsCas13b, CasRX, and EsCas13d in *Giardia*. pGDH= promoter of glyceraldehye 3-phosphate dehydrogenase (GL50803_6877). HA=Hemagglutinin-tag. *(C)* Schematic of CRISPRi vector dCas9g1pac and CasRX vector design. pMDH= promoter of malate dehydrogenase, pac=puromycin resistance marker, 2340NLS=GL50803_2340 nuclear localization signal, SCF=gRNA scaffold sequence, DR=Direct repeat for CasRX, pU6=*Giardia* U6 promoter. To determine if one of these knockdown systems might be better tolerated than the other, we examined the proportion of cells that expressed dCas9 or CasRX and found no appreciable difference. *(D)* Localizations of 3XHA tagged dCas9 and CasRX with DAPI staining in *Giardia*. *(E)* Quantification of cells with detectable dCas9 and CasRX expression. n.s.=not significant (p=0.70). Data are mean ± s.d. from three independent experiments (dCas9 n=3278, CasRX n=3327 cells) Mann-Whitney U-test. *(F)* Growth curve of dCas9 and CasRX expressing cell lines indicates that the growth rate is essentially identical for dCas9 and CasRX expressing cells. Blue=CasRX, Red=dCas9. Bars, 100 µm. To compare efficacy of knockdown, we designed CasRX- and CRISPRi-specific guide RNAs to deplete NanoLuc and CWP1. For these two genes CasRX outperformed CRISPRi reaching up to 80% reduction for CWP1. *(G-H)* Relative NanoLuc intensity of proteins targeted for knockdown with CRISPRi or CasRX gRNAs. Levels were normalized to non-specific gRNA controls. *(G)* Quantification of NanoLuc intensity of CWP1 (GL50803_5638), and *(H)* NanoLuc only. The expression levels is normalized to guide RNA controls. All experiments are from three independent biological replicates. Data are mean ± s.d. (n=3). Student's t-test, *p<0.01, **p<0.001, ***p<0.0001, ****p<0.00001, ns= not significant.

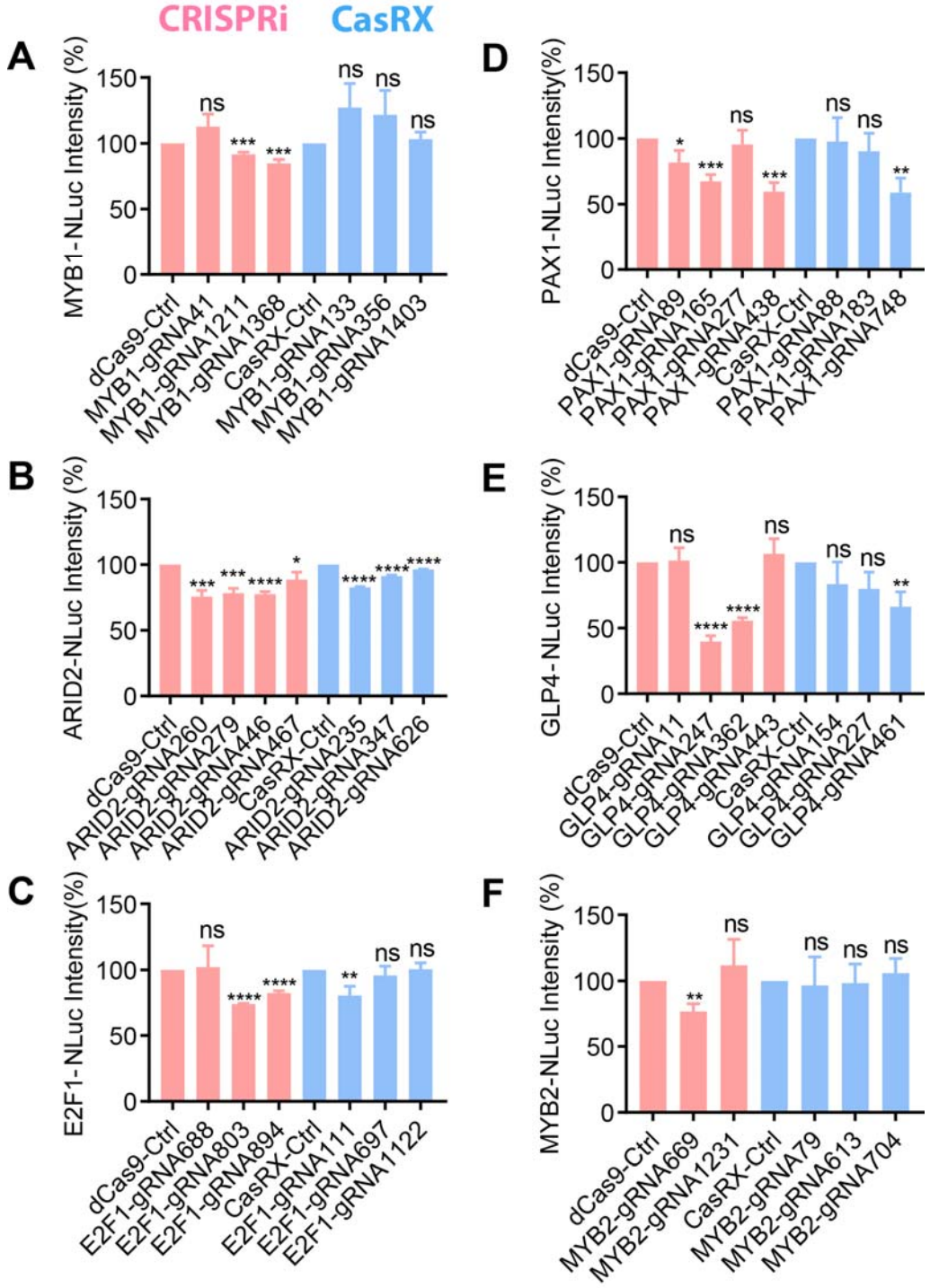

Fig. S4. Screen of guide RNAs with CRISPRi and CasRX systems. *(A-F)* Quantification of NanoLuc intensity using the indicated CRISPRi or CasRX guide RNAs. Levels were normalized to non-specific gRNA controls. *(A)* MYB1-NLuc (GL50803_5347). *(B)* ARID2-NLuc (GL50803_8102). *(C)* E2F1-NLuc (GL50803_23756). *(D)* PAX1-NLuc (GL50803_32686). *(E)* GLP4-NLuc (GL50803_33232). *(F)* MYB2-NLuc (GL50803_8722). All experiments are from three independent biological replicates. Data are mean ± s.d. (n=3) Student's t-test, *p<0.01, **p<0.001, ***p<0.0001, ****p<0.00001, ns= not significant.

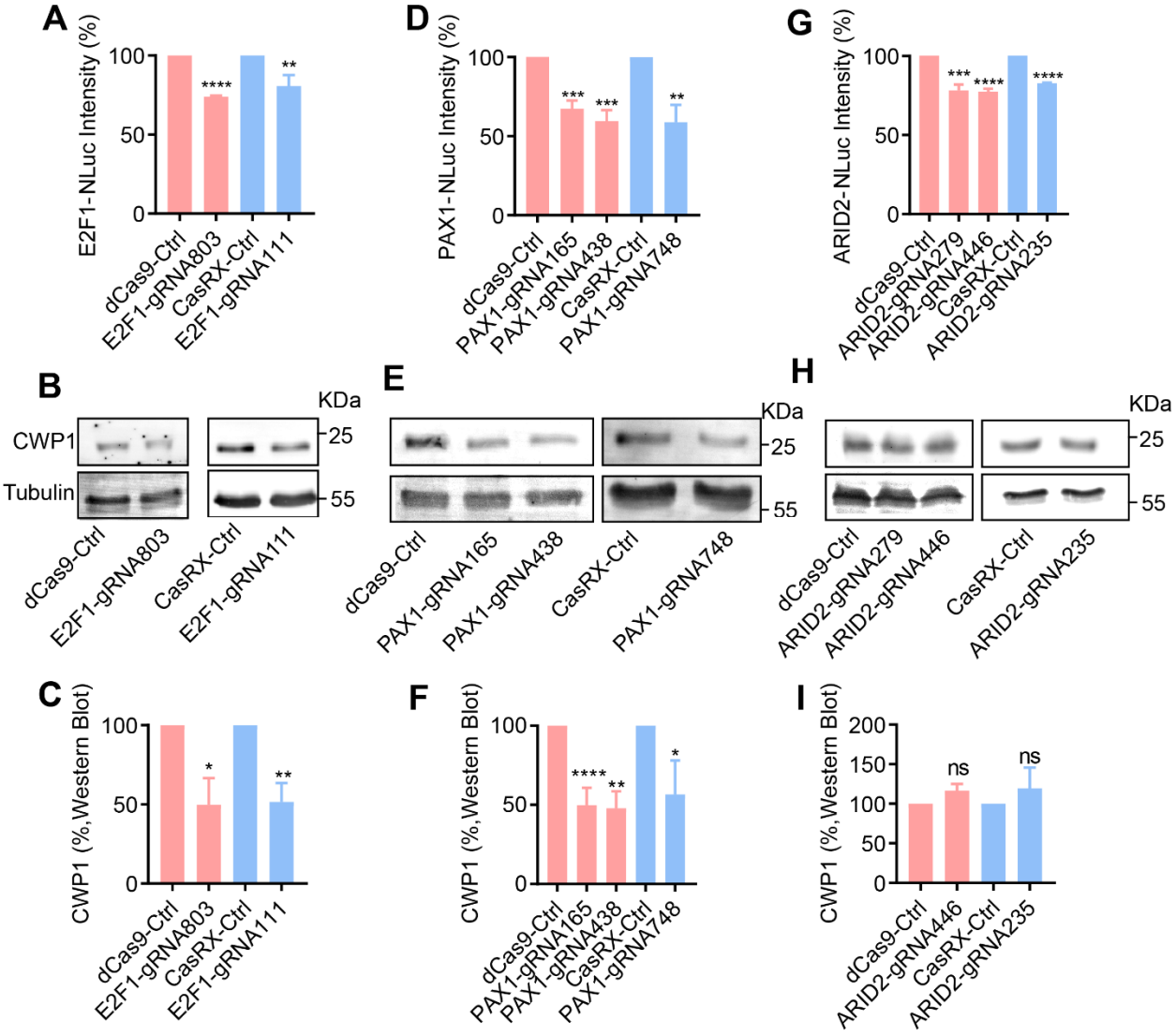

Fig. S5. Knockdowns of E2F1, PAX1, and ARID2 in *Giardia*. *(A,D,G)* Quantification of NanoLuc intensity from CRISPRi (or CasRX)-mediated knockdowns of (A) E2F1 (GL50803_23756), (D) PAX1 (GL50803_32686), and (G) ARID2 (GL50803_8102). The expression level is normalized to the corresponding dCas9 or CasRX control. *(B,E,H)* Western blots of CWP1 and tubulin from (B) E2F1, (E) PAX1, and (H) ARID2 knockdowns at 4 h of encystation. *(C,F,I)* Quantification of Western blots from (B) E2F1, (E) PAX1, and (H) ARID2 knockdowns, respectively. The expression level is normalized to the tubulin control. All experiments are from three independent biological replicates. Data are mean ± s.d. (n=3) Student's t-test, *p<0.01, **p<0.001, ***p<0.0001, ****p<0.00001, ns= not significant.

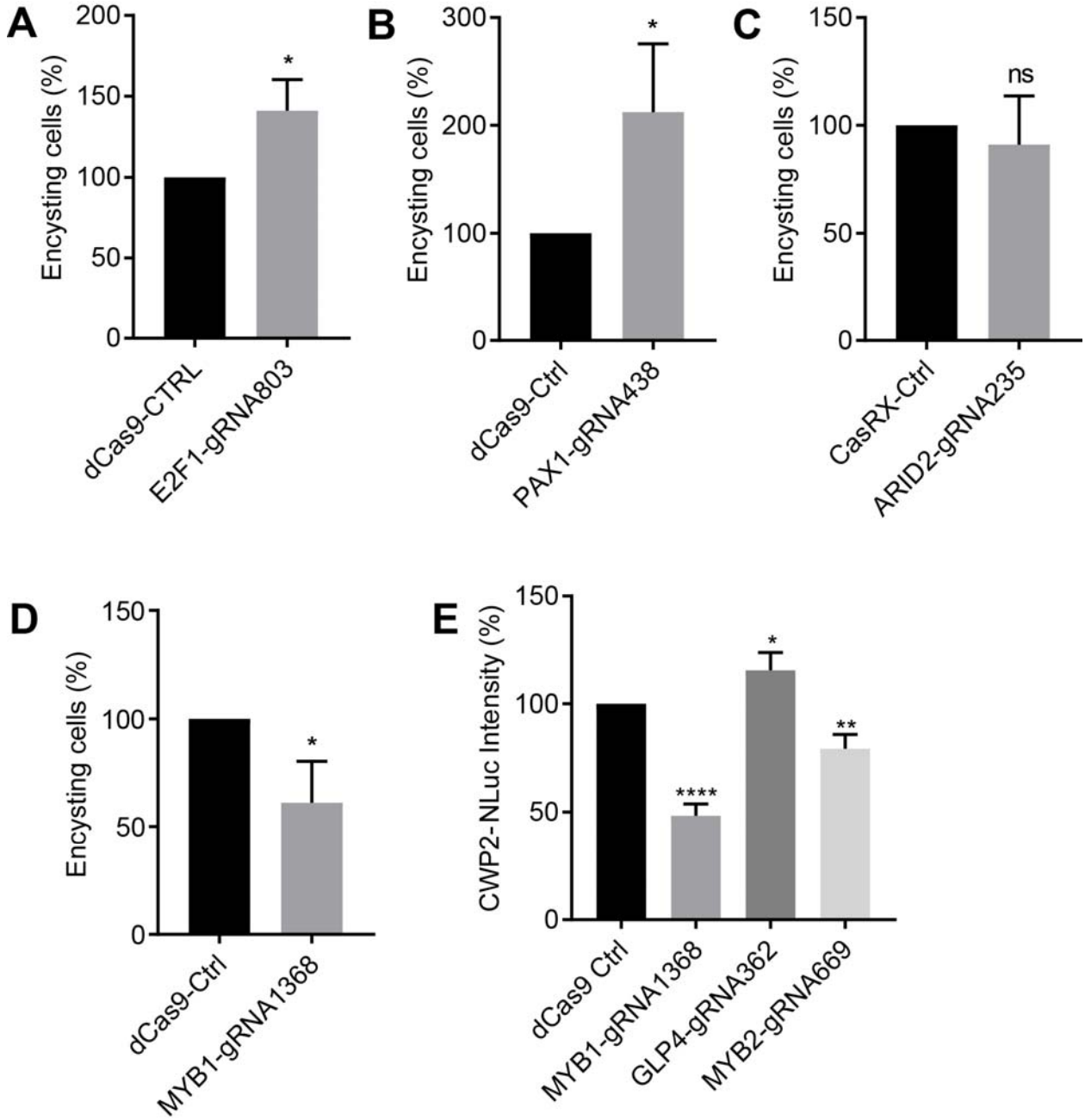

Fig. S6. Proportion of encysting cells in knockdowns of (A) E2F1, (B) PAX1, (C) ARID2, and (D) MYB1 at 4 h post induction of encystation. Data are mean± s.d. from three independent experiments (total cells counted for ***A***, dCas9-Ctrl n=626, E2F1-gRNA803 n=655; ***B***, dCas9-Ctrl n=638, PAX1-gRNA438 n=640; ***C***, CasRX-Ctrl n=625, ARID2-gRNA235 n=447 cells, **D**, dCas9-Ctrl n=428, MYB1-gRNA1368 n=356) Student's t-test, *p<0.01, **p<0.001, ****p<0.00001, ns= not significant. *(E)* Relative expression of CWP2 NanoLuc intensity in knockdowns of MYB1, MYB2 and GLP4 at 4 h post induction of encystation. The expression level is normalized to the dCas9 Ctrl. All experiments are from three independent biological replicates. Data are mean ± s.d. (n=3) Student's t-test, *p<0.01, **p<0.001, ****p<0.00001.

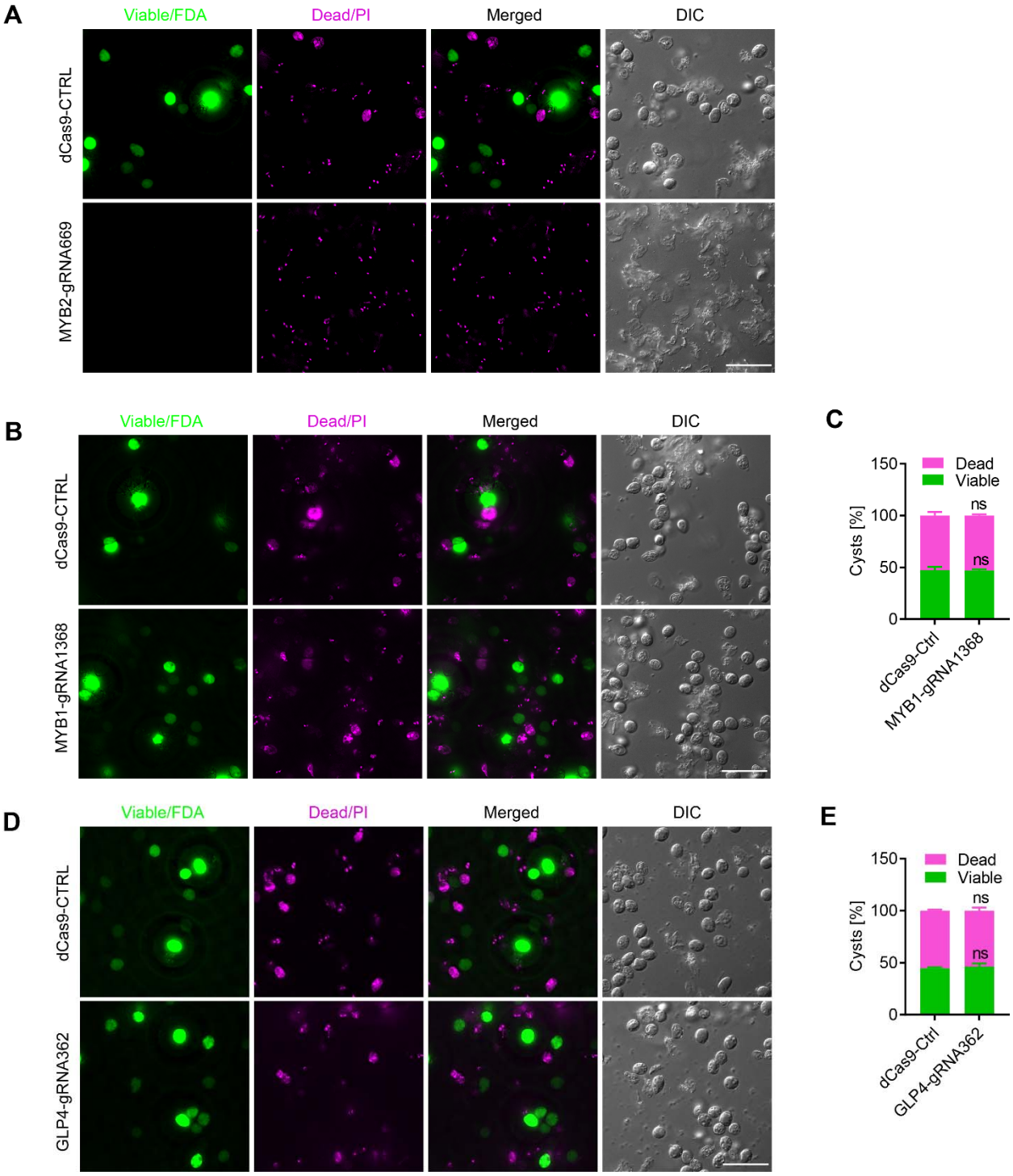

Fig. S7. Knockdown of GLP4 and MYB1 do not alter cyst viability. *(A)* MYB2-gRNA669 derived cysts stained with FDA (fluorescein diacetate, green=live) and PI (propidium iodine, magenta=dead) to determine cyst viability. *(B)* MYB1-gRNA1368 and (D) GLP4-gRNA362 derived cysts stained with FDA and PI. *(C)* Quantification of *(B). (E)* Quantification of (D). All cell lines were encysted for 48 h. Data are mean ± s.d. from three biological replicates (total cysts counted for dCas9-Ctrl n=400, GLP4-gRNA362 n=499, MYB1-gRNA1368 n=399) Student's t-test, ns= not significant. Bars, 100 µm.

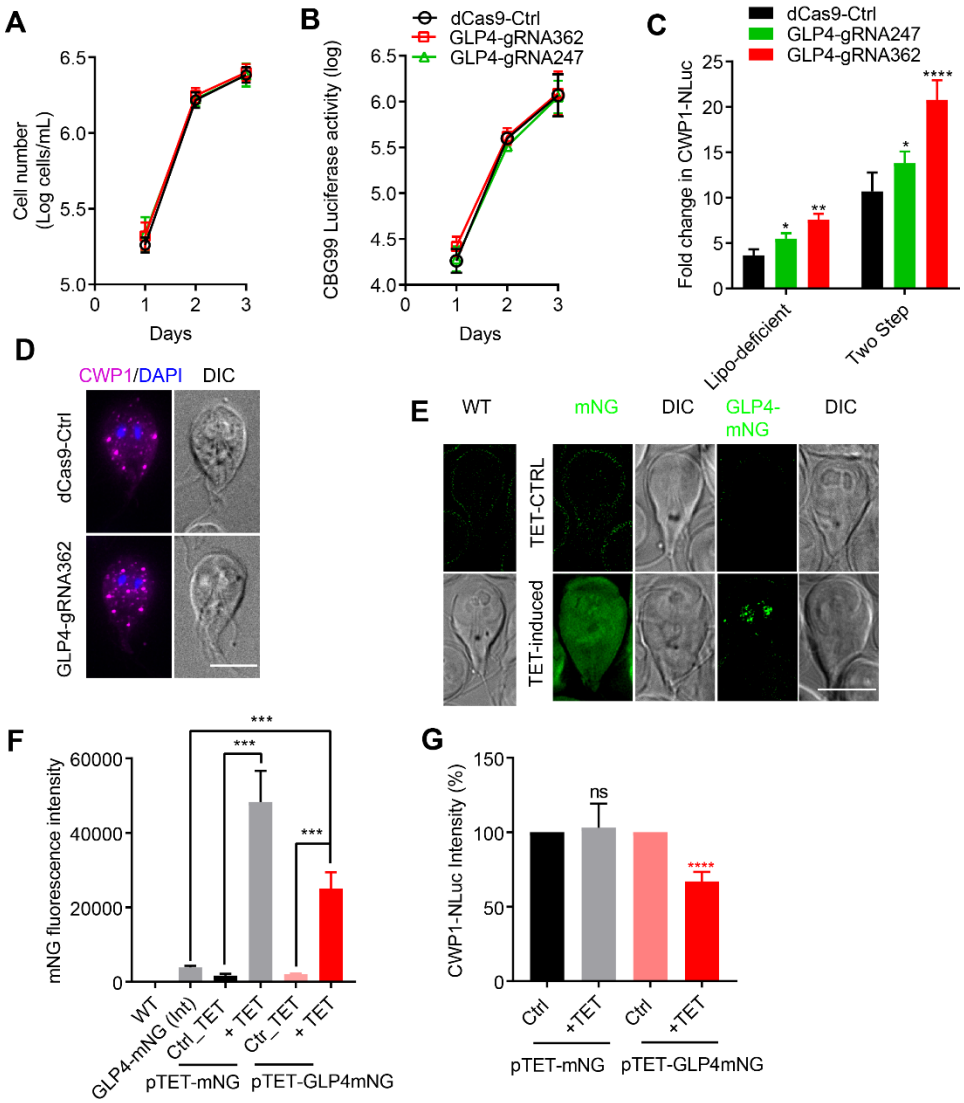

Fig. S8. Knockdown of GLP4 does not alter growth rate or cell viability. *(A)* Cell growth assay for dCas9 control and GLP4 knockdown strains. All cultures were started with 200,000 cells and then cell concentration was determined with a MOXI Z counter at 1, 2, and 3 days. *(B)* Cell viability of dCas9 control and GLP4 knockdowns at 1, 2, 3 days as determined by ATP dependent luminescence from CBG99. Three independent replicates of 200,000 cells/well were assayed in a plate reader. Black, dCas9 control. Red, GLP4-gRNA362. Green, GLP4-gRNA247. *(C)* Relative CWP1 NanoLuc intensity in GLP4 knockdowns at 4 h of encystation with lipoprotein-deficient medium or two step encystation medium. *(D)* Representative images of CWP1 stained vesicles in dCas9 control and GLP4-gRNA362 cell lines. *(E-F)* mNG expression images of WT, GLP4-mNG (Int) (integrated and endogenously tagged GLP4-mNG), pTET-mNG (mNG under the tetracycline inducible promoter) and pTET-GLP4-mNG (GLP4-mNG under the tetracycline inducible promoter) in the CWP1-NLuc background with or without tetracycline induction. All images were taken with same exposure. Bars, 10 µm. 20 µg/ml tetracycline (final concentration) was added to induce expression. *(F)* Quantification of (E). 2x 10^6 cells were assayed in each well of a clear-bottom black plate and mNG fluorescence intensity detected with a fluorescent plate reader. *(G)* Relative CWP1-NLuc intensity in mNG and GLP4-mNG overexpression cell lines at 4 h of encystation. Data are mean ± s.d. (n=3) Student's t-test, *p<0.01, **p<0.001, ****p<0.00001, ns=not significant.

712

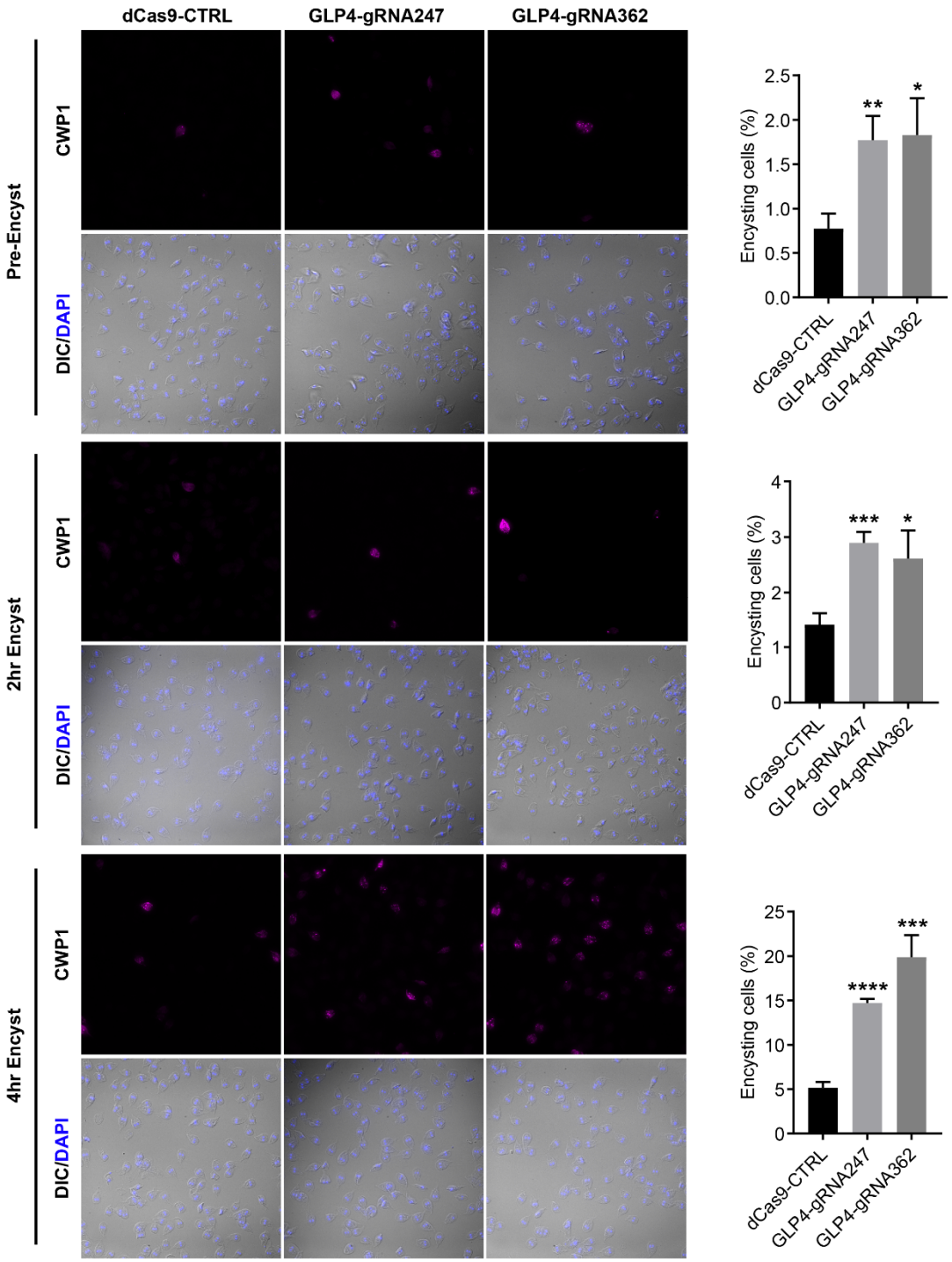

713 **Fig. S9.** Knockdown of GLP4 increases encystation rates. Quantification of CWP1 positives cells in control
714 and GLP4 knockdown strains at 0 h, 2h, and 4h post induction of encystation. Data are mean ± s.d. from
715 three biological replicates (total cells counted for 0 h: dCas9-Ctrl n=4927, GLP4-gRNA247 n=4927, GLP4-
716 gRNA362 n=5808; 2h: dCas9-Ctrl n=5785, GLP4-gRNA247 n=5785, GLP4-gRNA362 n=6041, 4 h: dCas9-
717 Ctrl n=5312, GLP4-gRNA247 n=5312, GLP4-gRNA362 n=4988 cells) Student's t-test, *p<0.01, **p<0.001,
718 ***p<0.0001, ****p<0.00001. Bars, 100 µm.

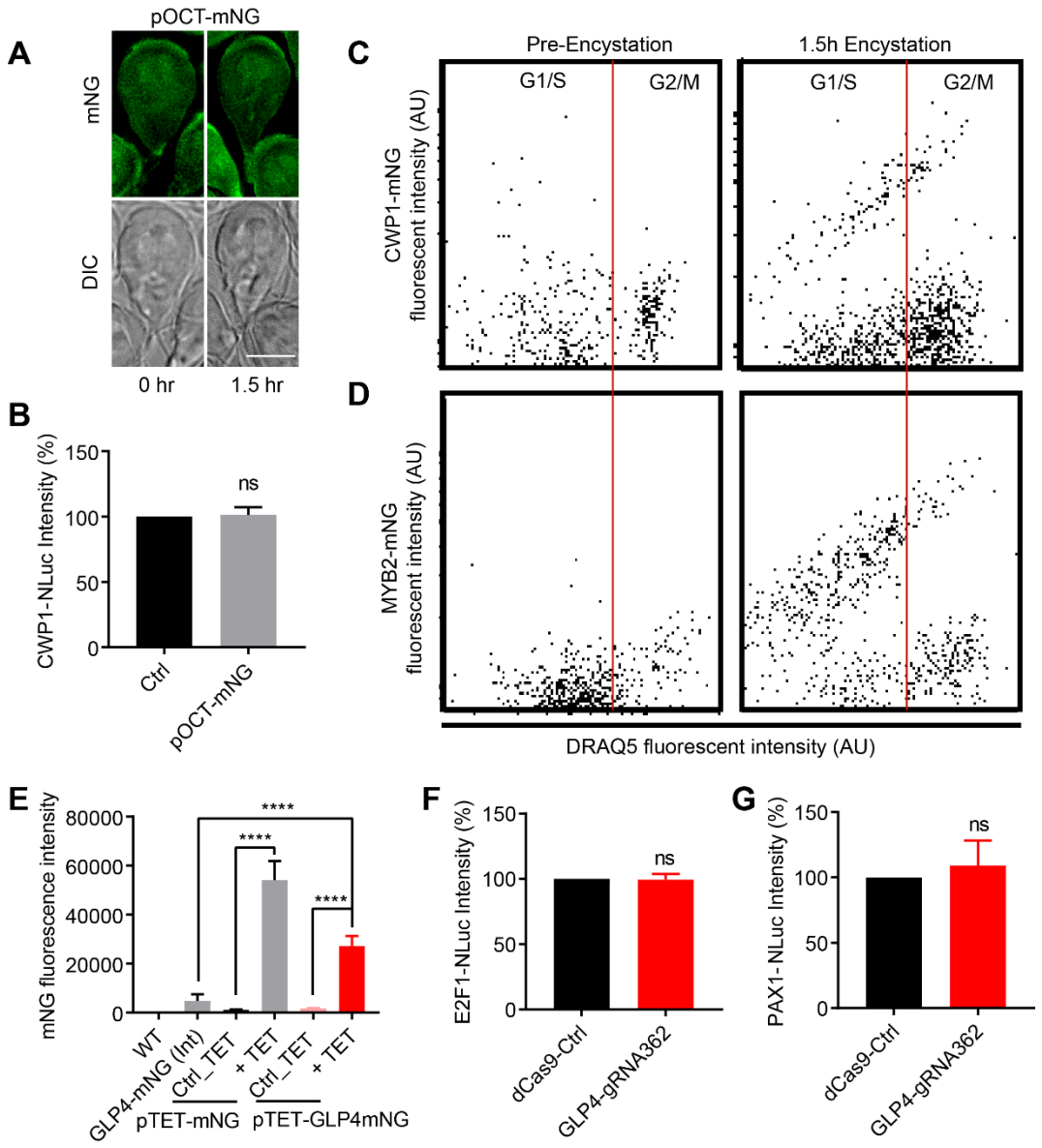

Fig. S10. G2+M cells have higher levels of CWP1 and MYB2. *(A)* Fluorescent images of the *p*OCT::mNG expressing cell lines at 1.5h post induction of encystation. pOCT=promoter of ornithine carbamoyltransferase (GL50803_10311), Bars, 10 µm. *(B)* Relative CWP1-NLuc intensity from *p*OCT-mNG cell lines at 4 h post induction of encystation. CWP1-NLuc intensity is normalized to the CWP1-NLuc parental line. Data are mean ± s.d. (n=3) Student's t-test, n.s.=not significant. *(C)* CWP1-mNG fluorescence intensity of DRAQ5-stained cells at 0 and 1.5 h of encystation. *(D)* MYB2-mNG fluorescence intensity of DRAQ5-stained cells at 0 and 1.5 h encystation. *(E)* mNG fluorescent intensity of WT, GLP4-mNG (Int) (integrated and endogenously tagged GLP4-mNG), *p*TET-mNG (mNG under the tetracycline inducible promoter) and *p*TET-GLP4-mNG (GLP4-mNG under the tetracycline inducible promoter) in the MYB2-NLuc cells with or without tetracycline induction. 20 µg/ml tetracycline (final concentration) was added to induce expression. Relative NanoLuc intensity of *(F)* E2F1 and *(G)* PAX1 levels in GLP4 knockdown cell lines at 4 h of encystation. Expression levels are normalized to the dCas9 control at 4h post induction of encystation. Bars, 10 µm. Data are mean ± s.d. (n=3) Student's t-test, *p<0.01, **p<0.001, ****p<0.00001, n.s.=not significant.

734 Table S1 Supplemental excel file containing all of the primer sequences used in this study.